

AD-A203 934

NAVAL POSTGRADUATE SCHOOL
Monterey, California



THESIS

SATELLITE SIGNATURES OF RAPID
CYCLOGENESIS

by

Jose F.H. Atangan

December 1988

Thesis Advisor

Carlyle H. Wash

Approved for public release; distribution is unlimited.

DTIC
ELECTE
FEB 14 1989
S H D

Unclassified

security classification of this page

REPORT DOCUMENTATION PAGE				
1a Report Security Classification Unclassified		1b Restrictive Markings		
2a Security Classification Authority		3 Distribution Availability of Report		
2b Declassification Downgrading Schedule		Approved for public release; distribution is unlimited.		
4 Performing Organization Report Number(s)		5 Monitoring Organization Report Number(s)		
6a Name of Performing Organization	6b Office Symbol (if applicable)	7a Name of Monitoring Organization		
Naval Postgraduate School	35	Naval Postgraduate School		
6c Address (city, state, and ZIP code)		7b Address (city, state, and ZIP code)		
Monterey, CA 93943-5000		Monterey, CA 93943-5000		
8a Name of Funding Sponsoring Organization	8b Office Symbol (if applicable)	9 Procurement Instrument Identification Number		
8c Address (city, state, and ZIP code)		10 Source of Funding Numbers		
		Program Element No	Project No	Task No
		Work Unit Accession No		
11 Title (include security classification) SATELLITE SIGNATURES OF RAPID CYCLOGENESIS				
12 Personal Author(s) Jose F.H. Atangan				
13a Type of Report	13b Time Covered	14 Date of Report (year, month, day)	15 Page Count	
Master's Thesis	From To	December 1988	59	
16 Supplementary Notation The views expressed in this thesis are those of the author and do not reflect the official policy or position of the Department of Defense or the U.S. Government.				
17 Cosat: Codes		18 Subject Terms (continue on reverse if necessary and identify by block number)		
Field	Group	Subgroup		
		Meteorology; Satellite Remote Sensing; Cloud Analysis		
19 Abstract (continue on reverse if necessary and identify by block number)				
<p>Animation of satellite visual and infrared imagery indicates that rapid cloud growth is a characteristic of explosively deepening cyclones. The working hypothesis in this thesis is that the intense vertical motions responsible for the low-level spin-up will produce rapid cloud expansion in the upper troposphere that can be detected using digital satellite data. Using digital IR data from GOES-West, the cloud growth of three explosive storms that developed over the eastern North Pacific Ocean were measured quantitatively and compared with the cyclone deepening rate. The results indicate that the growth in areal coverage of clouds colder than -45°C is most closely related to the explosive development period while the growth of the warmer cloud tops is related to the open wave stage. This relationship is dependent on the cloud pattern of the maturing cyclone. Correlations between cloud growth and pressure deepening were calculated but provide only a general estimate of the relationship between the two parameters. This study demonstrates the feasibility of using digitized satellite data to quantitatively analyze the cloud growth and structure of explosively developing cyclones.</p>				
20 Distribution Availability of Abstract		21 Abstract Security Classification		
<input checked="" type="checkbox"/> unclassified unlimited <input type="checkbox"/> same as report <input type="checkbox"/> DTIC users		Unclassified		
22a Name of Responsible Individual		22b Telephone (include Area code)	22c Office Symbol	
Carlyle H. Wash		(408) 646-2295	64Wx	

DD FORM 1473, 84 MAR

83 APR edition may be used until exhausted
All other editions are obsolete

security classification of this page

Unclassified

Approved for public release; distribution is unlimited.

Satellite Signatures of Rapid Cyclogenesis

by

Jose F.H. Atangan
Lieutenant, United States Navy
B.S., U.S. Naval Academy, 1981

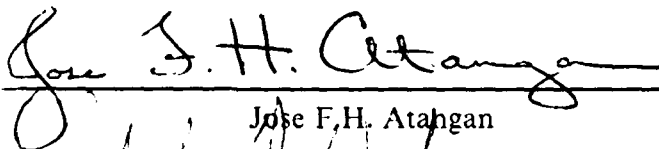
Submitted in partial fulfillment of the
requirements for the degree of

MASTER OF SCIENCE IN METEOROLOGY AND OCEANOGRAPHY

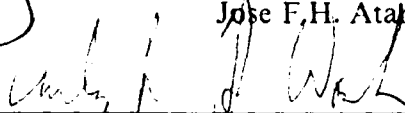
from the

NAVAL POSTGRADUATE SCHOOL
December 1988

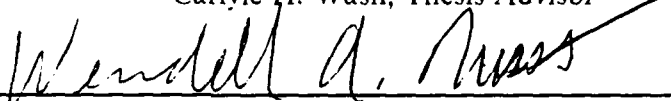
Author:


Jose F.H. Atangan

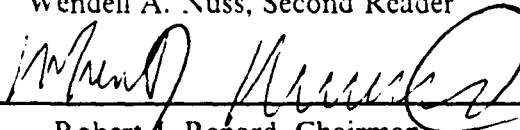
Approved by:



Carlyle H. Wash, Thesis Advisor



Wendell A. Nuss, Second Reader



Robert J. Renard, Chairman,
Department of Meteorology



Gordon E. Schacher,
Dean of Science and Engineering

ABSTRACT

Animation of satellite visual and infrared imagery indicates that rapid cloud growth is a characteristic of explosively deepening cyclones. The working hypothesis in this thesis is that the intense vertical motions responsible for the low-level spin-up will produce rapid cloud expansion in the upper troposphere that can be detected using digital satellite data. Using digital IR data from GOES-West, the cloud growth of three explosive storms that developed over the eastern North Pacific Ocean were measured quantitatively and compared with the cyclone deepening rate. The results indicate that the growth in areal coverage of clouds colder than -45°C is most closely related to the explosive development period while the growth of the warmer cloud tops is related to the open wave stage. This relationship is dependent on the cloud pattern of the maturing cyclone. Correlations between cloud growth and pressure deepening were calculated but provide only a general estimate of the relationship between the two parameters. This study demonstrates the feasibility of using digitized satellite data to quantitatively analyze the cloud growth and structure of explosively developing cyclones.



Accession For	
NTIS GRA&I	<input checked="" type="checkbox"/>
DTIC TAB	<input type="checkbox"/>
Unannounced	<input type="checkbox"/>
Justification	
By	
Distribution/	
Availability Codes	
Dist	Avail and/or Special
A-1	

TABLE OF CONTENTS

I. INTRODUCTION	1
II. BACKGROUND	3
III. DATA AND ANALYSIS	8
IV. RESULTS	11
A. CASE 1: 16-18 JANUARY 1988	11
1. Overview	11
2. Thresholding Results	13
B. CASE 2: 14-16 DECEMBER 1987	22
1. Overview	22
2. Thresholding Results	22
C. CASE 3: 1 - 2 JUNE 1988	33
1. Overview	33
2. Thresholding Results	33
D. SUMMARY	43
V. CONCLUSIONS AND RECOMMENDATIONS	45
LIST OF REFERENCES	47
INITIAL DISTRIBUTION LIST	49

LIST OF TABLES

Table 1.	STORM DATES AND CENTRAL PRESSURE STATISTICS.	8
Table 2.	THRESHOLD PIXEL COUNTS AND TEMPERATURES	10
Table 3.	COLOR SCHEME FOR IR IMAGE ENHANCEMENTS	10

LIST OF FIGURES

Fig. 1. Central pressure evolution	12
Fig. 2. IR imagery for 0546 UTC 16 January 1988	13
Fig. 3. IR imagery for 1746 UTC 16 January 1988	14
Fig. 4. Storm track for 16-17 January 1988	15
Fig. 5. Cloud growth: 00 UTC 16 January 1988- 00 UTC 18 January 1988.	16
Fig. 6. IR imagery enhancement: 0600 UTC 16 January 1988	18
Fig. 7. IR imagery enhancement: 0000 UTC 17 January 1988	19
Fig. 8. IR imagery enhancement: 1500 UTC 17 January 1988	20
Fig. 9. Cloud growth: 00 UTC 16 January 1988-00 UTC 18 January 1988	21
Fig. 10. Central pressure evolution	23
Fig. 11. GOES imagery: 1346 UTC 14 December 1987.	24
Fig. 12. GOES imagery: 1546 UTC 15 December 1987.	25
Fig. 13. Storm track: 14 - 17 December 1988.	26
Fig. 14. Cloud growth: 14 - 15 December 1987.	27
Fig. 15. IR image enhancement:1200 UTC 14 December 1987.	28
Fig. 16. IR image enhancement:0000 UTC 15 December 1987.	29
Fig. 17. IR image enhancement:1500 UTC 15 December 1987.	30
Fig. 18. IR image enhancement:0000 UTC 16 December 1987.	31
Fig. 19. Central pressure evolution	34
Fig. 20. GOES imagery: 1746 UTC 1 June 1988.	35
Fig. 21. GOES imagery: 0546 UTC 2 June 1988.	36
Fig. 22. Storm track: 1 - 3 June 1988.	37
Fig. 23. Cloud growth: 1 - 2 June 1988.	38
Fig. 24. IR image enhancement:1800 UTC 1 June 1988.	39
Fig. 25. IR image enhancement:0300 UTC 2 June 1988.	40
Fig. 26. IR image enhancement:1200 UTC 2 June 1988.	41
Fig. 27. IR image enhancement:2000 UTC 2 June 1988.	42

ACKNOWLEDGEMENTS

I wish to express my gratitude and appreciation to the following people who provided encouragement, guidance and assistance throughout this study. Professor Carlyle Wash, who conceived the project and gave outstanding guidance, counseling and assistance essential to its completion. Professor Wendell Nuss, for his critical review of this thesis. Rick Kohrs, for his assistance in the IDEA Lab and for providing the color image enhancements. Special thanks to Craig Motell for his tireless efforts on my behalf. Craig authored the computer programs used to process and analyze the digital data and kept me believing that I could complete this project. Most importantly, I would like to thank my wife, Renee, and my son, Daniel, for their love, support and understanding.

I. INTRODUCTION

One of the many challenges facing meteorologists today is the improvement of maritime weather prediction. A key aspect of this challenge is understanding the nature of rapidly intensifying cyclones. These systems present considerable danger to shipping, fixed ocean platforms and near-coastal regions. The combined effects of high winds, heavy seas and reduced visibility developing over short periods of time has resulted in substantial property damage, injury and loss of life. A recent example of the destructive nature of such rapidly developing systems is the storm that struck southern England on 15-16 October 1987. The gale force winds associated with this storm were directly responsible for 18 fatalities and millions of dollars of property damage (Burt and Mansfield, 1988).

Sanders and Gyakum (1980) defined rapid cyclogenesis as central pressure falls of at least 1 mb h for 24 h (normalized with respect to 60°N). In a detailed study involving a three year sample of North Atlantic and North Pacific Ocean systems, they found explosive cyclones to be a predominantly maritime, cold season event with hurricane strength wind fields. Included in their sample was the storm which damaged the luxury liner *Queen Elizabeth II* and sunk another vessel on 10 September 1978. Most of these storms were found to develop in areas of strong sea-surface temperature gradients, such as those associated with the Gulf Stream and Kuroshio currents. They also found that explosive deepening is a characteristic of the vast majority of the deepest cyclones in the Northern Hemisphere.

Numerous studies of explosive cyclogenesis events conducted in the past decade have improved our understanding of the dynamic and thermodynamic processes of explosive development. However, current numerical models have had only limited success in predicting their occurrence. It has been suggested by a number of authors (Tracton, 1973; Sanders and Gyakum, 1980; Bosart, 1981; Gyakum, 1983a,b; Anthes, et al., 1983) that the reason operational models fail to adequately forecast the observed rapid deepening rates may be due partially to their inability to simulate the bulk effects of cumulus convection on the cyclone's development. Other factors, such as poor horizontal and vertical resolution, inadequate model planetary boundary layer structure (Bosart, 1981), poor initial conditions (Reed and Albright, 1986) are also important.

Rogers and Bosart (1986) emphasize that a major problem in studying rapid cyclogenesis is their oceanic location, where regularly reporting rawinsonde stations are rare. This lack of data makes conventional studies of synoptic and mesoscale features of explosive cyclones difficult and at times impossible. As a result, it has been difficult to investigate the physical and dynamical atmospheric processes that produce explosive development.

Satellite imagery has become a critical tool in the analysis of tropospheric weather systems, and cyclones in particular. The use of satellite imagery of ocean storms has been limited primarily to subjective analysis. Animation of visual and infrared images has indicated that rapid cloud growth is a characteristic of explosively-developing cyclones. The working hypothesis in this thesis is that the intense vertical motions responsible for the low-level spin-up will produce rapid cloud expansion in the upper troposphere that can be detected using digital satellite data. The objective of this study is to demonstrate the feasibility of using digitized satellite imagery data to analyze quantitatively the cloud structure of explosive cyclones and to study relationships between cloud growth and cyclone deepening.

Chapter II presents a review of cyclone signature studies. Data for this study and the method of analysis are discussed in Chapter III. The results of each case study and a summary are presented in Chapter IV, followed by conclusions and recommendations in Chapter V.

II. BACKGROUND

Early research on the use of satellite imagery as an aid to analysis and forecasting focused on the use of satellite observed cloud patterns in the interpretation of synoptic patterns, particularly the positioning of surface fronts and lows and the likelihood of cyclogenesis. From these early studies, Anderson et al. (1973) prepared typical cloud models describing the development of low-level baroclinic cyclones at 24 h intervals. These models made it possible to extrapolate a cloud pattern from a current image to a pattern as it would appear the following day. In their study, cyclogenesis within 24 h was indicated by: (1) the increase in the width of a cloud band associated with the warm front; (2) an increase in the vertical thickness of clouds in the same region; (3) the appearance of anticyclonic curvature of the main cloud band on the cold air side; and (4) the appearance of mesoscale streaks of upper and mid-level clouds along the anticyclonically-curved boundary of the cloud mass.

In addition, Anderson et al. described a cloud pattern associated with positive vorticity advection (PVA). They showed that when this pattern interacts with a baroclinic cloud band, cyclogenesis often occurred. Wave formation began when a comma cloud, reflecting a maximum of PVA approached a frontal band. As the comma cloud continued to intensify, cyclonic circulation increased at low levels, resulting in a more northerly flow in the cold air behind the vorticity center and more southerly flow of the warmer air ahead of the PVA area.

Cloud patterns for each stage of cyclone development were also used by Troup and Stretten (1972) in an early attempt to use satellite imagery to estimate central pressures of extratropical storms. Anomaly values were determined by categorizing each cloud pattern. These anomaly values were then combined with mean sea-level charts to arrive at an estimate of the storm's central pressure. This system is a useful guide for manual and numerical analysis over sparse or no-data areas such as the Southern Hemisphere, but was subject to large errors due partially to the large standard deviations of the mean sea-level pressures.

The patterns outlined by Anderson et al. (1973) were used by Bottger et al. (1975) to compare a characteristic cloud shape associated with explosive cyclones with those of normal development. In a statistical investigation of 22 explosive cyclone developments in the period of 1968-1973, Bottger et al. utilized ESSA polar orbiter imagery to

show that satellite imagery can be used to arrive at an improved 24 h prognosis even when numerical models fail to give indications of explosive development. They found that explosive development was often preceded by the appearance of a solid cloud configuration called a head cloud. No cloud heads occurred without being followed by a major deepening at the surface. Their study indicated that the formation of the cloud head can precede explosive development by 24-36 h. A continual evolution of the head cloud pattern was not investigated because the use of ESSA imagery allows only one visual observation per day.

Bottger et al. relate the cloud head formation to a normal cyclogenetic process involving a condition of extreme baroclinicity along a front between subpolar and subtropical air masses. The cloud head formation is also described by Fett and Bohan (1981) as consisting of a compact, anticyclonically-curved cirrus and multiple layer cloud canopy centered over the surface disturbance and surrounded by a large field of open cellular cumulus on the cold air side. Additional characteristics include an anticyclonically-curved cirrostratus shield that covers the entire system in which the associated degree of curvature is dependent on the stage of development and a sharp northern boundary of the shield coincides with the jet stream axis. These characteristics appear in the early stages of deepening when only a weak wave is discernible on the surface pressure analysis.

An example of a typical rapidly developing cyclone as viewed in geostationary satellite imagery is presented by Burtt and Junker (1976). Using Synchronous Meteorological Satellite II (SMS-II) data, they note that two clues usually signify a rapidly deepening storm. First, a V-shaped dry wedge forms in the rear of the bright clouds, directly behind the surface low. This formation is in response to substantial cold air advection and sinking motions at low and mid levels. When a system begins rapid development, subsidence is large and cumulus development is suppressed within the slot. Secondly, in response to strong PVA, jet-associated cirrus forms a pattern that turns from cyclonic to anticyclonic near the location of the surface wave. Their description of this cloud system closely matches that of a head cloud described by Bottger et al. (1975). Burtt and Junker (1976) state that the availability of satellite data and the regular occurrence of the aforementioned patterns makes satellite imagery a valuable tool for forecasting explosive development.

The cloud pattern evolution of oceanic cyclogenesis is further discussed by Weldon (1977). He refers to the earliest detectable characteristic of the incipient cyclone cloud pattern for many cases of cyclogenesis as a "baroclinic leaf". Although there are many

variations of the baroclinic leaf, Weldon describes the pattern as generally having a sharp, well defined northern edge with a low amplitude "S" shape and a relatively uniform cloud top area. He notes that the intensification of a system is indicated by an increase in the definition of the northern edge and uniformity of the cloud top area. This increase in definition is often accompanied by the dissipation of cloudiness adjacent to the main cloud area leaving a multi-layered head cloud formation. Subsequent evolution reveals the disappearance of the band at the poleward edge and the development of a comma-like cloud. Weldon (1979) indicates that the baroclinic leaf is a pattern associated with frontogenesis aloft within a westerly windfield that extends to the surface. He observed that the subsequent evolution of the baroclinic leaf is influenced by the strength of the surface frontal zone and can include complex upper-level patterns which have multiple jet structures.

Weldon (1979) also described and categorized the cloud patterns representing winter storms approaching their lowest central pressure either at the surface or in the middle troposphere at about 700 mb. He noted that, although storms often grow larger beyond this stage, the central pressure does not get much lower and the strong pressure gradients retreat from the center. His observations were made using IR data.

The first cloud pattern for a mature winter storm described by Weldon (1979) was labeled as Type A. The Type A cloud pattern is characterized by a thick deck of cirrostratus clouds with a well defined, anticyclonically-curved northern and western edge. This cirrus deck often partially overlies a comma cloud pattern that is in its later stage. Generally, the cloud tops of the comma cloud are at middle levels; however, these systems are often highly convective and some cirrus level cumulus tops are involved. In almost all cases, where the back edge of the cirrus deck crosses the comma cloud, the comma cloud are at distinct lower level.

The second category of cloud patterns in mature winter storms is the Type B. The primary difference between the two categories is the configuration of the cirrostratus deck. Unlike the Type A, where the back edge of the cirrostratus deck crosses over the lower level comma cloud, the Type B cirrostratus deck wraps around the circulation center. The comma cloud associated with the Type B pattern normally appears behind the cirrostratus deck but in some cases their rear edges may coincide.

A case study of a baroclinic development is provided by Jager (1984). He observed that rapid cyclogenesis is indicated by the presence of anticyclonically-curved cirrus bands in a region where the jet stream has a cyclonic curvature. He notes that these high clouds will later assume the baroclinic leaf shape. His study shows that rapid

cyclogenesis can occur when the leaf overtakes an existing frontal system, especially one with a wave on the front. He concludes that the appearance of the baroclinic leaf in satellite imagery is a reliable indicator of strong surface cyclogenesis and can be useful in evaluating prognostic charts.

Junker and Haller (1980) developed a system for assigning central pressures to low centers based on the amount of circulation that can be seen in satellite visible and infrared imagery. Their study focused on developing cyclones in regions of strong baroclinicity during the period from October to April, when temperature gradients are greatest and baroclinic development is at its peak. Comparing satellite images of cyclones with characteristic curving cloud patterns to corresponding surface analyses, Junker and Haller found that distinct cloud patterns could be associated with six pressure groups between 1000 and 960 mb.

This system provides meteorologists with a means of estimating surface pressures of cyclones when no surface observations are available. However, this system applies only to a specific subset of extratropical storms and is limited by its seasonality. Additionally, it does not account for lows whose surface pressure is already below 1000 mb when cyclogenesis begins and should be confined to areas north of 40 ° N. Smigielski and Ellrod (1985) suggests that the system can be modified for these cases by adjusting each pressure group by a factor corresponding to the difference between 1000 mb and the pressure at which cyclogenesis begins.

Williams (1985) conducted a study of the satellite-observed cloud patterns of explosive cyclones in the western North Atlantic Ocean. He confirmed the findings of Weldon (1977 and 1979) that the first stages of storm development usually consist of baroclinic leaf-type developments and the appearance of the head cloud described by Bottger et al. (1975) precedes explosive development by 24 to 36 hours. Williams (1985) concluded that these distinct cloud patterns are strong indicators of explosive development. However, a developmental model utilizing these patterns could not be formulated because of a wide variety of cloud pattern sequences.

The use of satellite imagery in analysis of synoptic weather patterns has increased dramatically in recent years. Improvements in available communication systems has increased the accessibility and the quality of satellite data. Although the data are available in digital form, analysis has been limited to subjective analysis as outlined by Anderson et al. (1973) and others. Burfeind and Weiman (1987) demonstrate that quantitative analysis of meteorological imagery of extratropical storms is feasible. Using the classification scheme developed by Troup and Stretten (1972), a computerized pattern

analysis technique was developed to locate and classify features of mature extratropical storms. They conclude that computers can conduct quantitative analyses of satellite imagery that gives results comparable to those obtained by human analysts using subjective analysis techniques. The goal of this thesis is to study additional quantitative cloud measurements that apply to rapid cyclogenesis events.

III. DATA AND ANALYSIS

This study investigates three storms that developed over the eastern North Pacific Ocean. The dates and pressure statistics for these storms are shown in Table 1. The central pressures were obtained from the National Meteorological Center final surface analyses available in the archives of the Department of Meteorology, Naval Postgraduate School, Monterey, California.

Table 1. STORM DATES AND CENTRAL PRESSURE STATISTICS.

Date	Initial Pressure (mb)	Lowest Pressure (mb)	Rate of fall (mb/h) Normalized to 60° N
14-17 Dec 87	1011	978	2.0
16-18 Jan 88	1008	987	1.4
1-3 Jun 88	1006	968	2.0

The digital satellite data for the December and January storms were obtained from the Departments of Meteorology of the University of Wisconsin and Colorado State University. To examine the feasibility of using data that are routinely available to operational facilities, the data for the June storm were obtained using the PC MCIDAS software package utilized in the Naval Postgraduate School's Meteorology/Oceanography Interactive Digital Environmental Analysis (IDEA) Laboratory. The satellite data sets consist of hourly infrared imagery obtained from the VAS (VISSR¹ Atmospheric Sounder) instrument flown aboard the GOES-West and GOES-East satellites. The infrared data were from the VAS sensor's Channel 8 which has a central wavelength of 11.2 μ m.

The nominal ground spatial resolution of the University of Wisconsin and Colorado State University data is 4 km at the satellite sub-point. The nominal resolution of the PC MCIDAS data at the sub-point is considerably less at 8 km. The difference in resolution can be attributed to the technique used in processing the raw data from the satellite.

¹ Visible and Infrared Spin Scan Radiometer

The VAS sensor measures pixels with a nominal resolution of 8 X 4 km. That is, the pixel has a height of 8 km corresponding to the line spacing and width of 4 km corresponding to the element spacing. Unfortunately, when displaying images it is necessary to have square pixels. To correct this problem, each line is displayed twice in the vertical, thus giving the appearance of a pixel element with a resolution of 4 X 4 km. This technique is used by the University of Wisconsin and Colorado State University to obtain the full resolution IR data used in this study. The PC MCIDAS software uses a similar technique but duplicates only every other line resulting in an image covering a larger area but having lower resolution.

Images covering the storms' development over a period of at least 24 h prior to the storms' mature stage are examined. The areal coverage of clouds in the upper troposphere for various temperature thresholds is calculated from the digital data. The processing utilized a program which consists of three steps; 1) selecting the cloud area, 2) selecting the pixel count associated with a temperature threshold and 3) counting the number of pixels of the selected pixel count.

The thresholding area is a rectangular sector of variable dimensions encompassing the system of interest. The dimensions of the thresholding area were established using imagery of the storm's mature stage. The boundaries of the thresholding area were defined simply as the edges of the brightest clouds of the vortex. The size of the thresholding area is kept constant for all images to ensure that any changes that can be detected are due to the storm's development rather than changes to the thresholding area.

Full resolution GOES data as displayed in the IDEA Laboratory have a radiometric resolution of 8 bits equating to 256 gray levels. Each level is referred to as a pixel count and is related to black body temperature. This relationship is obtained from enhancement curves provided in the header information that is unique to each data set. For this study, the enhancement curves from the different data sets were found to be identical for the pixel counts of interest.

Therefore, the choice of pixel count corresponds to a choice of cloud temperature. Because the interest of this study is in the highest clouds, pixel counts corresponding to the coldest cloud top temperatures were investigated. The pixel counts and the corresponding temperatures used in this study are shown in Table 2.

Once the pixel count has been selected, pixels representing temperatures greater than the corresponding temperature value of the selected pixel count are discarded. The number of pixels remaining in the thresholding area are counted to yield a numerical

representation of cloud areal coverage. The result of the thresholding process is a new data set consisting of the areal coverages of clouds of a given temperature threshold for the developing cyclone. The cloud area growth is then determined from these statistics. The cloud growth curves are compared with a plot of the storm's deepening rate to determine possible relationships.

Table 2. THRESHOLD PIXEL COUNTS AND TEMPERATURES

Pixel Count	Temperature (° C)
205	-60
200	-55
190	-45
180	-35
164	-25
144	-15

Color image enhancements were also generated to determine the location of the cloud growth with respect to the position of the low and to visually verify the cloud growth reflected in the cloud growth curves. Because the thresholding area cannot completely prevent the contribution of clouds outside of the system of interest, these enhancements also proved helpful in estimating the amount of cloud growth that should not be considered part of the storm's development. Table 3 provides a listing of the enhancement colors and the temperature ranges used in the results of the satellite analysis that follows in Chapter IV.

Table 3. COLOR SCHEME FOR IR IMAGE ENHANCEMENTS

TEMPERATURE RANGE (° C)	COLOR
< -60	Black
-55 to -59	Purple
-45 to -54	Blue
-35 to -44	Yellow
-25 to -34	Orange
-15 to -24	Red

IV. RESULTS

A. CASE 1: 16-18 JANUARY 1988

1. Overview

This subsection describes the movement and development of Case 1. The discussion is based on the NMC final surface analyses and GOES-West imagery covering the period from 0000 UTC 16 January 1988 thru 0000 UTC 18 January 1988.

This storm can be categorized by three stages of development during this period:

1. Open wave stage (0000-1800 UTC 16 January 1988)
2. Explosive stage (1800 UTC 16 January 1988 - 1500 UTC 17 January 1988)
3. Mature stage (1500 UTC 17 January 1988 - 0000 UTC 18 January 1988).

These stages are similar to the stages of explosive cyclone development described by Rogers and Bosart (1986).

The stages of development are best illustrated by the evolution of the central pressure shown in Fig. 1. During the open wave stage little change in central pressure was evident. This stage was characterized by the presence of a shortwave disturbance indicated by the appearance of a comma shaped cloud in the GOES imagery west of a frontal wave. In the infrared imagery for 0600 UTC 16 January 1988 (Fig. 2), the comma cloud located at 40° N, 155° W approaches a frontal band associated with a quasi-stationary front. By 1800 UTC 16 January 1988, the comma cloud has interacted with the frontal band to form a head cloud (Fig. 3), signalling the onset of explosive deepening.

The explosive stage of development represents a period of intense deepening. This period is characterized by the 21 mb pressure drop from 1008 mb to 987 mb in 21 hours shown in Fig. 1. During this period, the storm evolves from a head cloud formation into a tightly wrapped spiral. By 1500 UTC 17 January 1988 the storm has reached the mature stage of development and has formed a Type B cloud pattern for mature winter storms described by Weldon (1979). The pressure drop and growth of the storm ceases.

The movement of the storm (Fig. 4) follows a predominantly eastward track. For the open wave stage of development the position of the comma cloud was used to

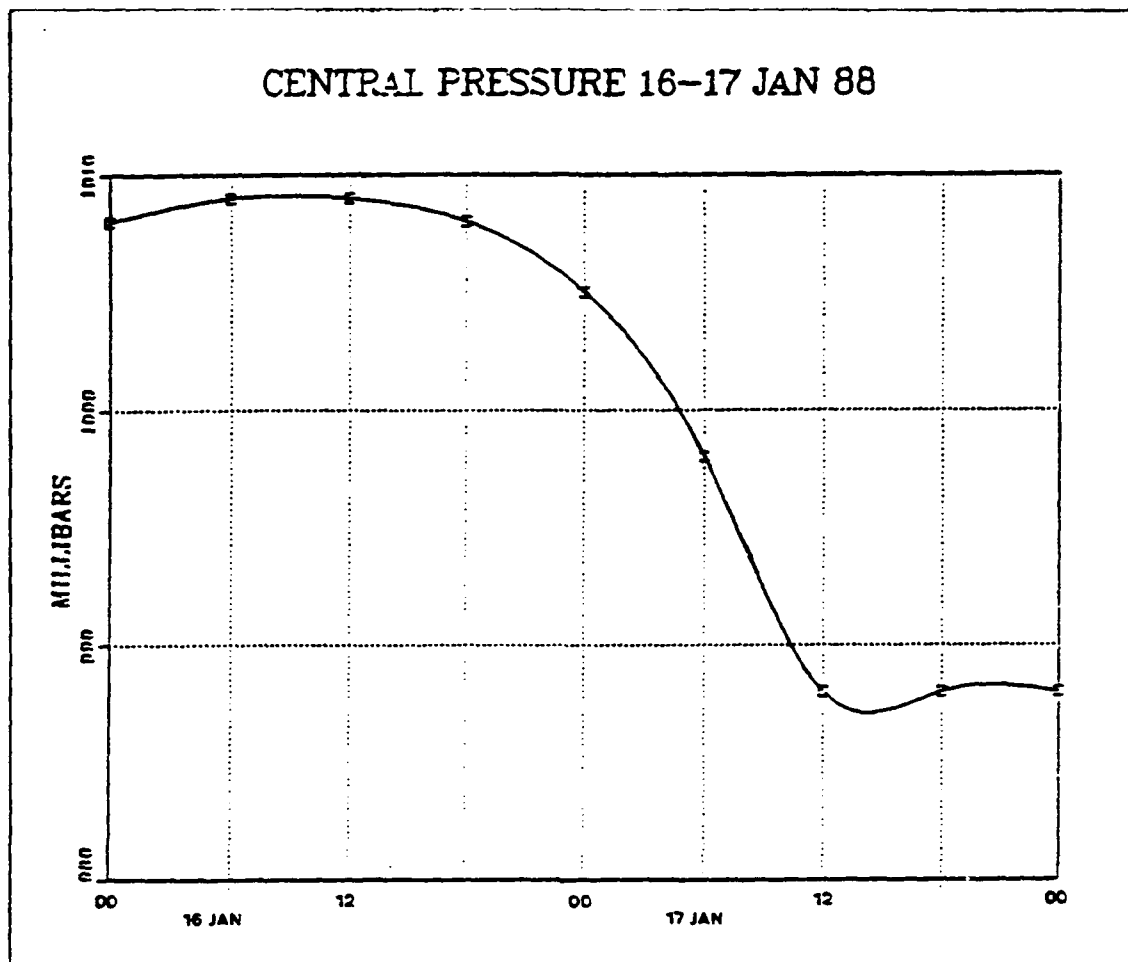


Fig. 1. Central pressure evolution: 00 UTC 16 January 1988 - 00 UTC 18 January 1988.

determine the storm track because the absence of a sea-level pressure center. The central pressures for this period were based on the sea-level pressure below the comma cloud. During the open wave stage, the comma cloud moved in a southeastward direction until 1800 UTC 16 January 1988 when it merged with the frontal band and a low of 1008 mb was formed, marking the beginning of the explosive stage. In the initial phase of the explosive stage the storm moved rapidly to the east-northeast at an average speed of approximately 100 km/h over a 6 h period. By 0600 UTC 17 January 1988 the low had deepened to a central pressure of 998 mb and alters course to the east-southeast. This course was maintained through the mature stage although the storm slows to 40 km/h as it approaches the California coast.

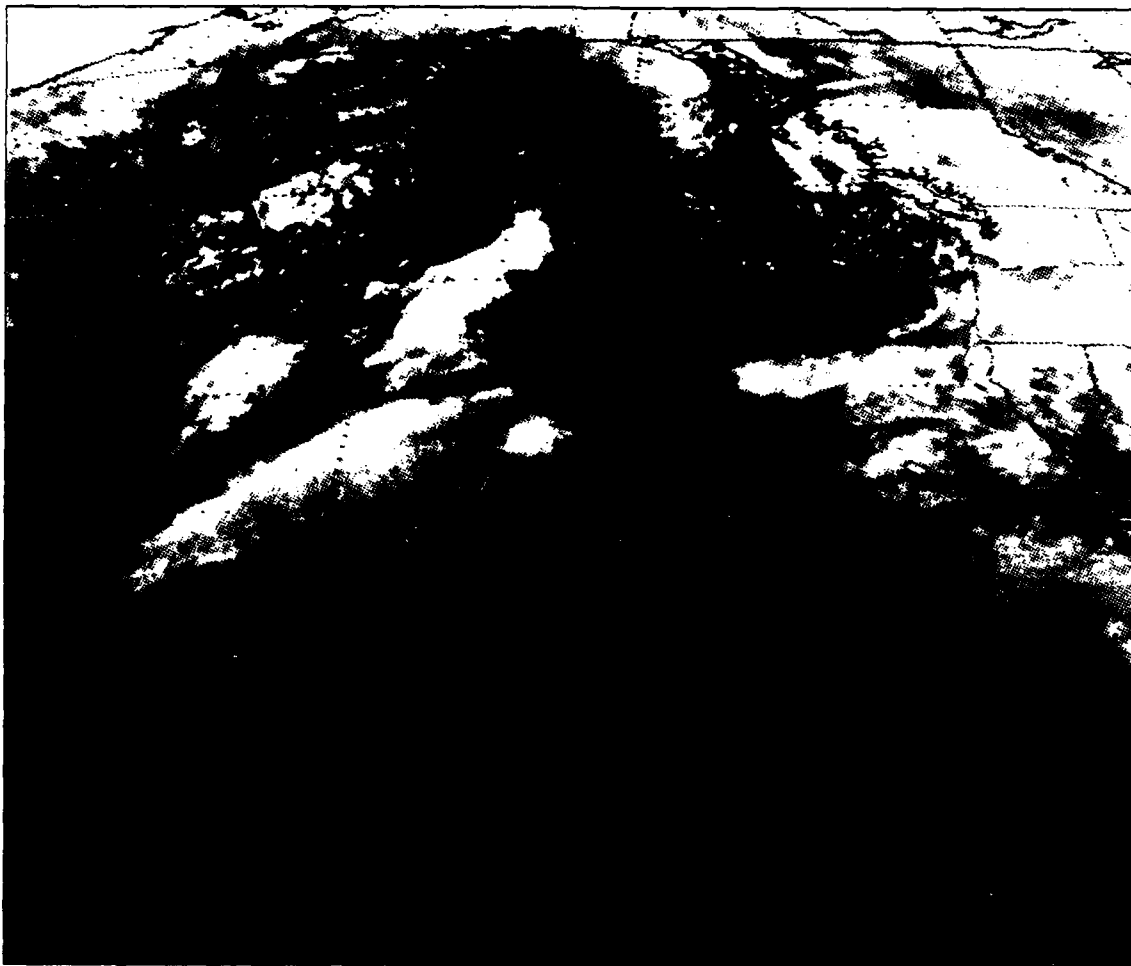


Fig. 2. IR imagery for 0546 UTC 16 January 1988

2. Thresholding Results

The dimensions of the thresholding area used in this case were 250 pixels in the north-south direction and 400 pixels in the east-west direction. This equates to a rectangular region approximately 1700 km by 2500 km when centered at 35° N. The dimensions of the thresholding area were established to adequately cover the cloud field of the storm during its mature stage and kept constant throughout the entire process to ensure the cloud growth reflected is due to storm development and not resulting from changes in the thresholding area.

The results of the thresholding process are graphically presented in Fig. 5. The figure presents a time series of the number of pixels associated with each temperature threshold used. The number of pixels represents all pixels for temperatures less than or

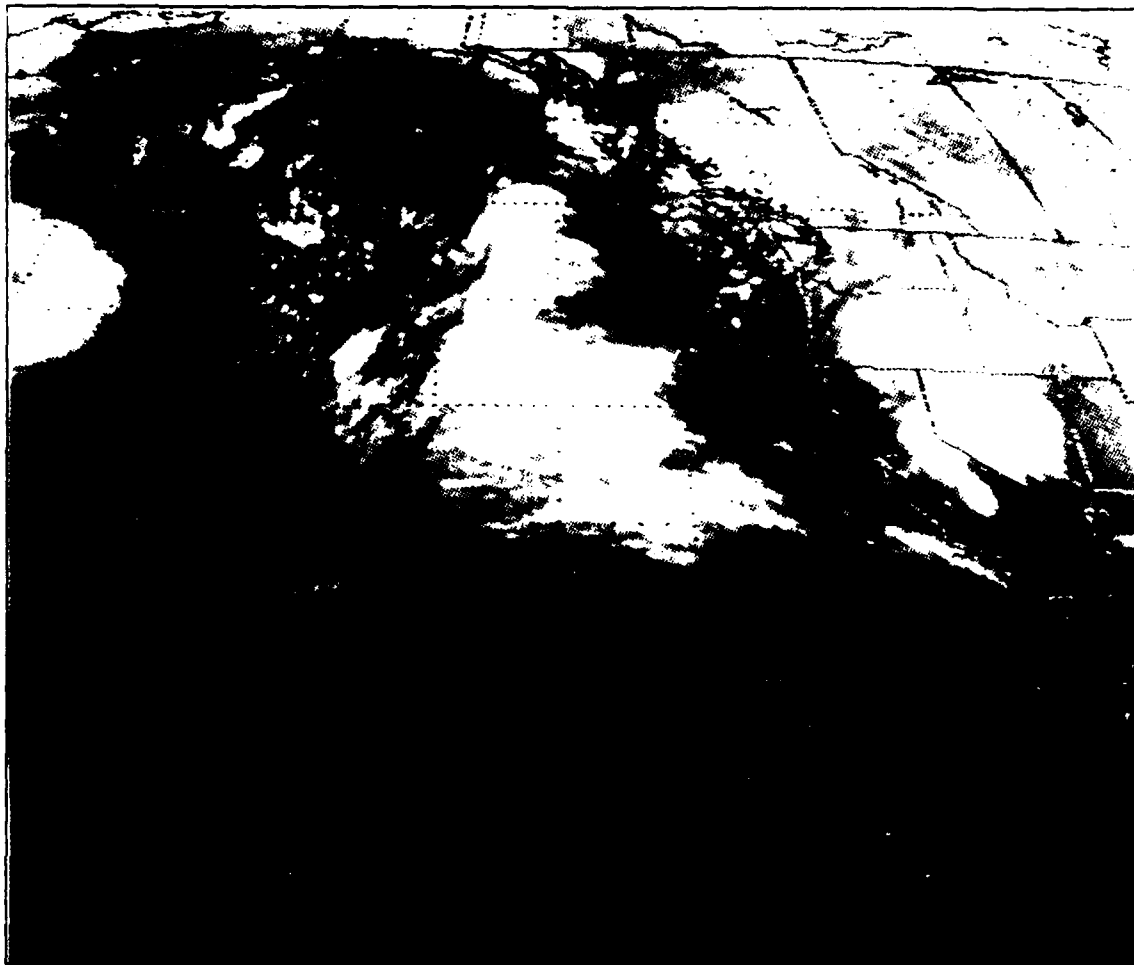


Fig. 3. IR imagery for 1746 UTC 16 January 1988

equal to the selected temperature threshold. Because the movement of the storm was primarily to the east, changes in the number of pixels may be directly associated to changes in cloud areal coverage.

The curves representing temperature thresholds of -15°C , -25°C and -35°C show similar cloud growth tendencies throughout the analysis period. In the open wave stage of development when only small changes in central pressure were analyzed (Fig. 1), the curves show a noticeable increase in cloud area which continues for approximately 9 h after the onset of explosive deepening. For the remainder of the analysis period the tendency becomes less clear due to large fluctuations in the pixel number.

The cloud growth tendencies in Fig. 5 are further illustrated through the use of color enhancements of the IR imagery (Fig. 6 - Fig. 8). The thresholding area is

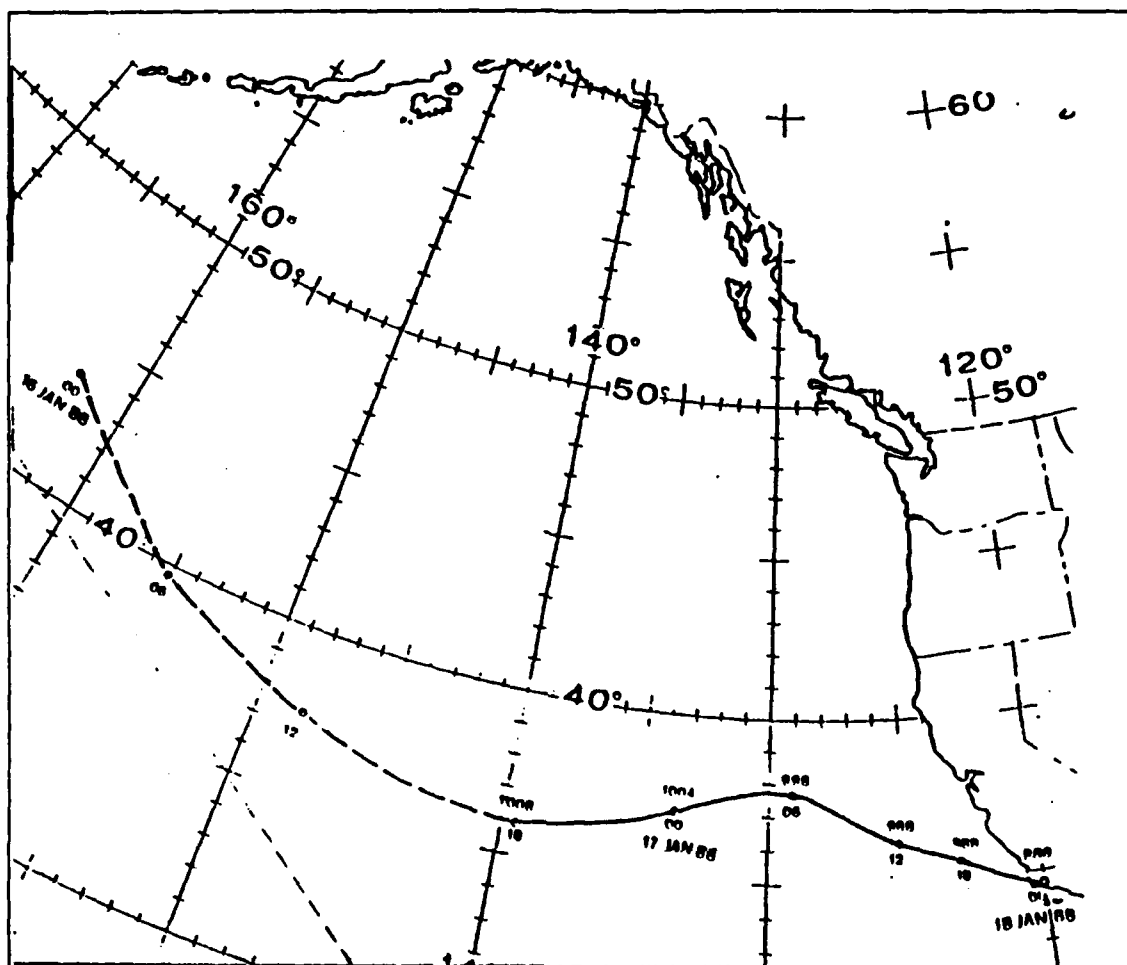


Fig. 4. Storm track for 16-17 January 1988: Dashed line indicates open wave stage of development. Solid line indicates explosive and mature stages.

outlined in each of the enhancements. The enhancement of the 0600 UTC 16 January 1988 shows a comma cloud in the northwest section of the thresholding area approaching a frontal wave band. The temperature of the comma cloud tops are generally colder than -35°C . The frontal band is characterized by a large region of cloud tops colder than -25°C with cloud tops colder than -35°C dominating the poleward edge of the band. In the northeast section of the thresholding area, a fraction of another comma cloud is visible. Although this comma cloud also interacts with the frontal band, it develops independently from the explosive event. Microwave satellite data from the Defense Meteorological Satellite Program for 1600 UTC 16 January 1988 studied by Sheridan (1988) shows a distinct separation in the precipitation activity between the

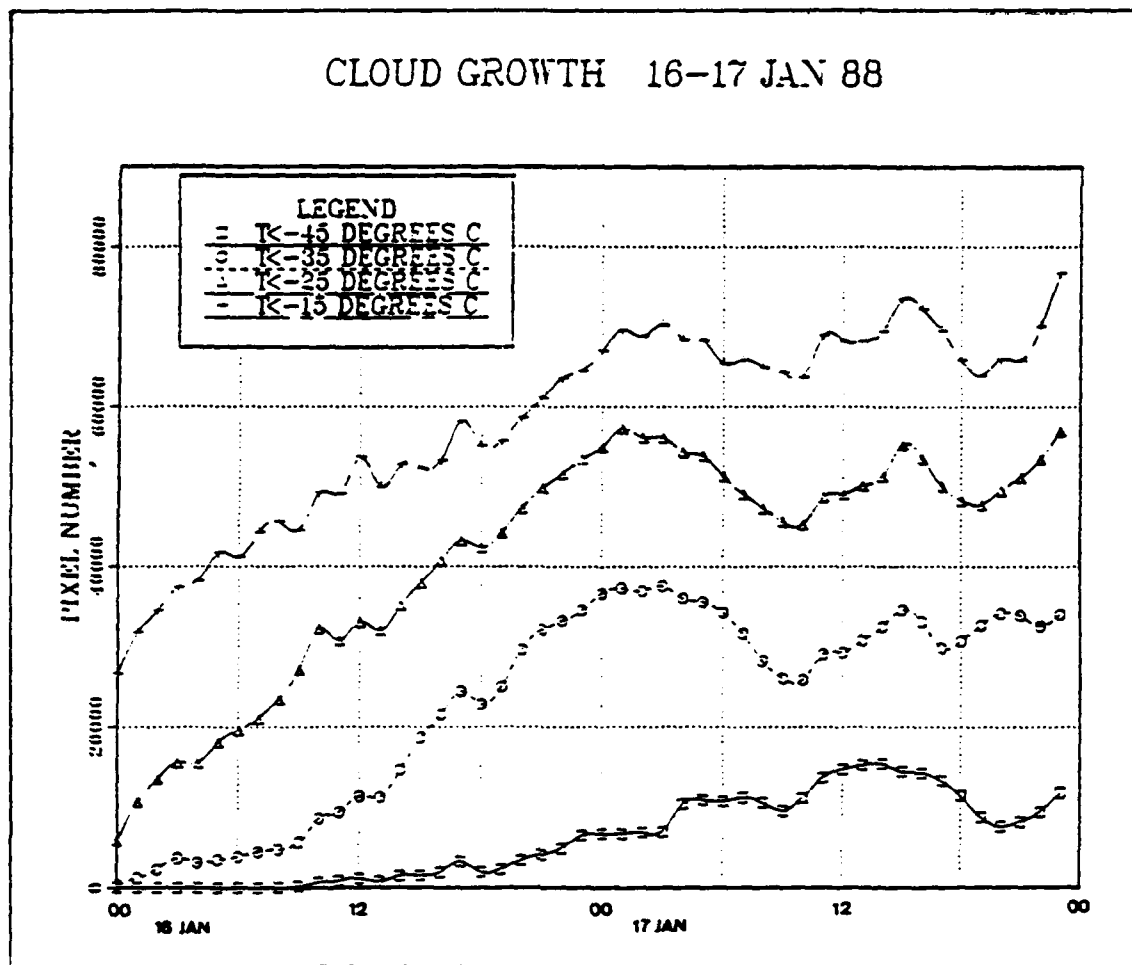


Fig. 5. Cloud growth: 00 UTC 16 January 1988- 00 UTC 18 January 1988.

northern cloud band and the developing cyclone. However, because the cloud masses merge during their development it is difficult to completely isolate the cloud fields of the explosive event, using IR data, particularly in the early stages. This results in the contribution of a some pixels by clouds that are not part of the system of interest.

At 0000 UTC 17 January 1988, the storm is in the early phase of the explosive stage, with a central pressure of 1004 mb. The image enhancement for this time (Fig. 7) shows that the merger of the comma cloud and frontal band is complete. The majority of the cloud tops are colder than -35°C . Comparing this enhancement with the 0600 UTC 16 January 1988 enhancement (Fig. 6) reveals a significant increase in the areal coverage of clouds colder than -45°C . This increase is also reflected in the cloud growth curves (Fig. 5) which shows the number of pixels representing a temperature

threshold of -45°C increasing from a negligible amount to 6674 pixels, nearly 22% of cloud tops colder than -35°C . These curves also reveal that by 0000 UTC 17 January 1988 the areal coverage of cloud tops with temperature thresholds of -15°C , -25°C and -35°C has reached its maximum extent. There is still some contribution from cloud masses not associated with the explosive event but this contribution has decreased and is now limited to the northwest corner of the thresholding area.

By 1500 UTC 17 January 1988 the storm reaches maturity with a central pressure of 987 mb. The cloud field forms a spiral vortex that is characteristic of a fully developed cyclone. A key feature revealed by the imagery enhancement (Fig. 8) is the large area of cloud tops colder than -45°C . The greatest concentration of these cloud tops were located above the occlusion area to the northeast of the surface center. When compared to the previous image enhancements, it is easy to see that there is a dramatic increase in the areal coverage of clouds with a threshold temperature of -45°C .

The coldest cloud tops are most closely related to the rapid development period. A closer examination of the growth of cloud tops colder than -45°C is possible by expanding the scale of the pixel number axis in the cloud growth curves (Fig. 9). Comparing the expanded curve (Fig. 9) with the evolution of the central pressure (Fig. 1) reveals that at the beginning of the analysis period there were no cloud tops with temperatures colder than -45°C . During the open wave stage of development a modest increase to nearly 2000 pixels occurs between 0600 and 1800 UTC 16 January 1988 while the central pressure showed only a slight drop of 1 mb. The increase in the number of pixels is large in the explosive stage when the number of pixels rises from 1934 to over 15000. The curve also shows that the maximum extent of the cloud growth occurred at approximately 1500 UTC 17 January 1988, the same time the storm reached its deepest pressure of 987 mb. This is followed by a dramatic reduction in pixel number to nearly half of that seen at its peak by 2000 UTC 17 January 1988.

The results of this case reveal a strong relationship between cloud growth and cyclone deepening. For temperature thresholds of -15°C , -25°C and -35°C a steady increase in cloud area was most apparent during the open wave stage of development with only small changes of central pressure. For a threshold temperature of -45°C the most rapid increase in cloud area occurred during the period of explosive deepening and the maximum extent of the areal coverage occurred when the storm reached its deepest pressure. The enhancements reveal that the greatest concentration of cloud tops colder than -45°C was located above the occlusion and confirm the cloud growth indicated in the cloud growth curve.

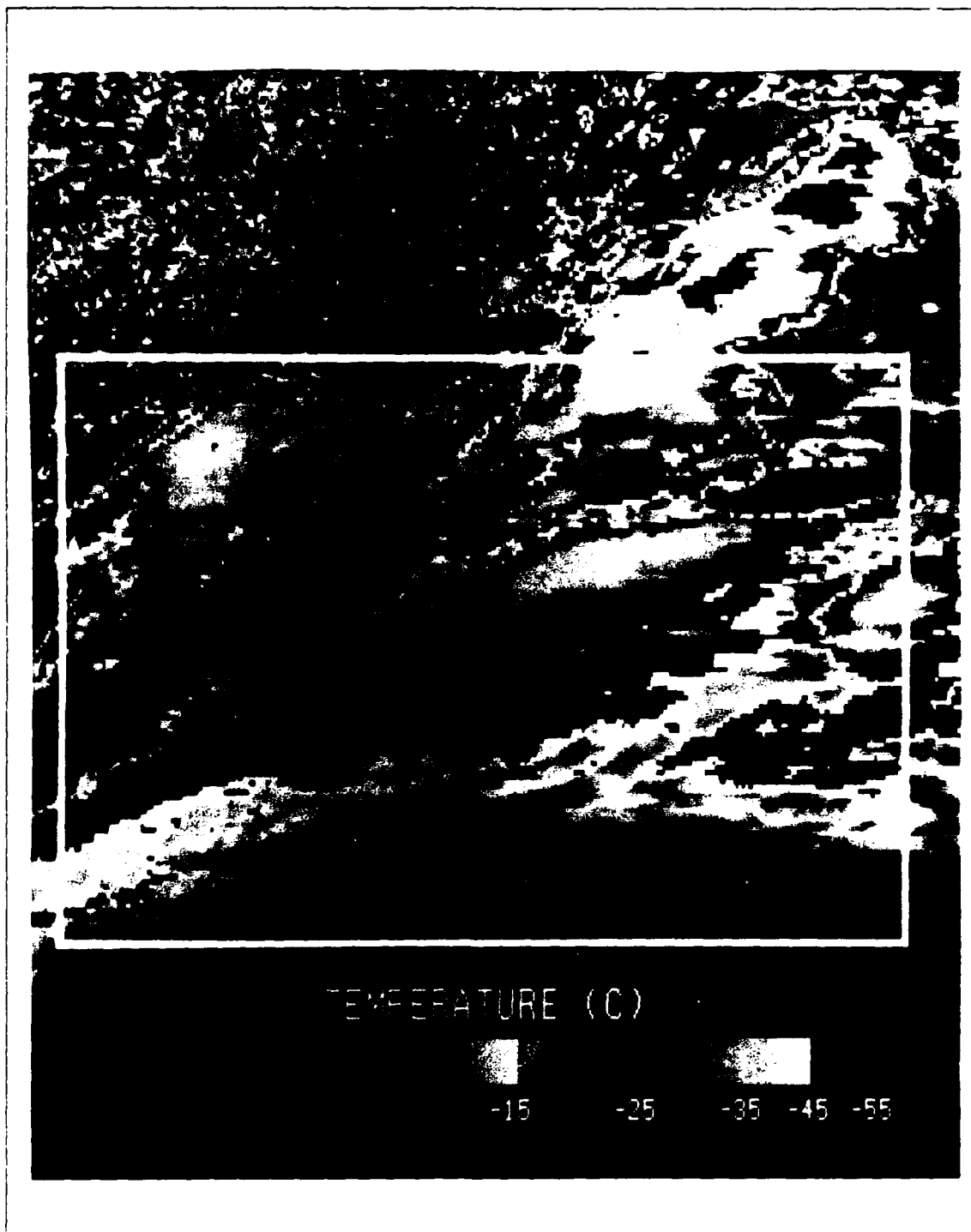


Fig. 6. IR imagery enhancement: 0600 UTC 16 January 1988: The boundaries of the thresholding area are outlined by the white lines.



Fig. 7. IR imagery enhancement: 0000 UTC 17 January 1988: The boundaries of the thresholding area are outlined by the white lines.

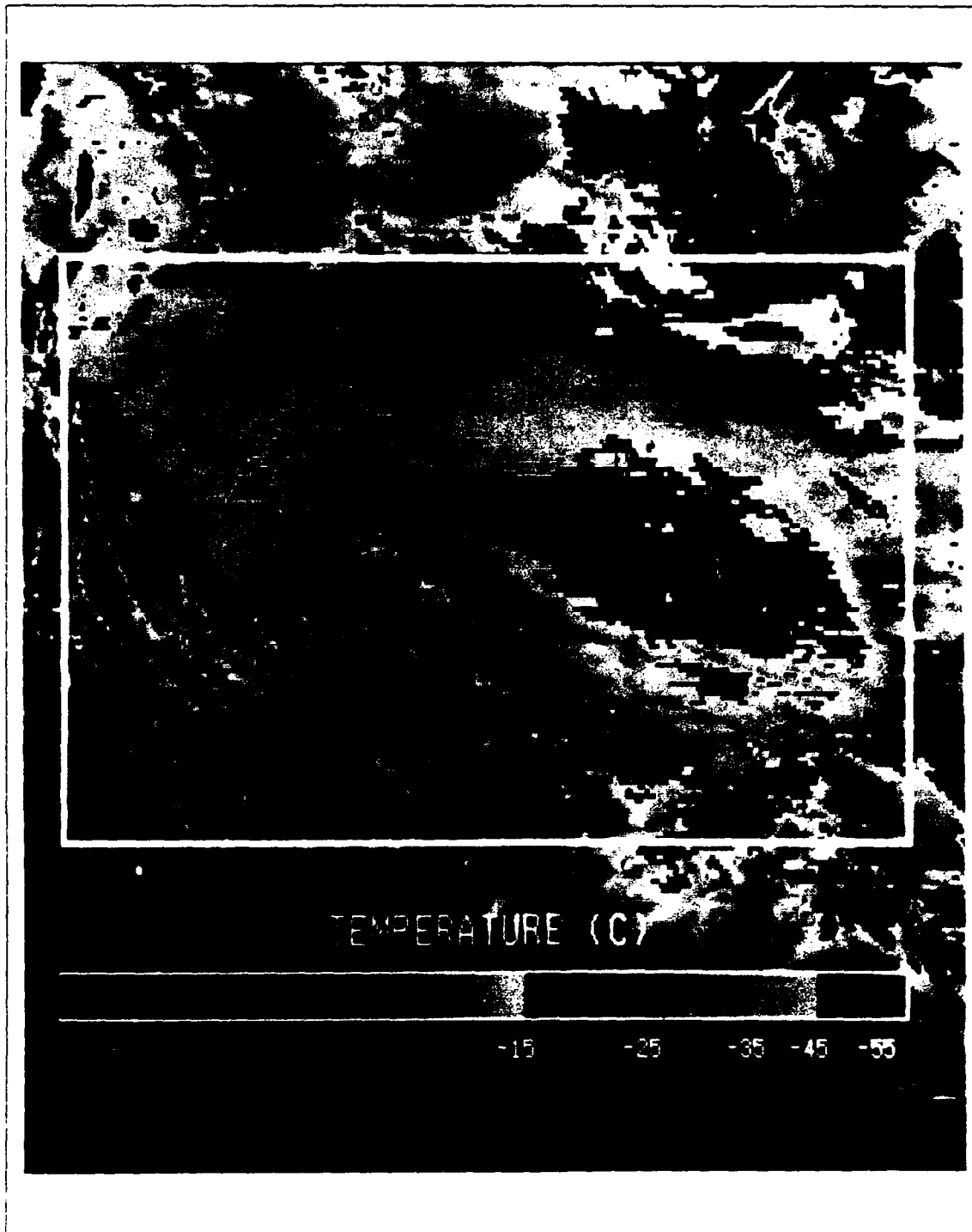


Fig. 8. IR imagery enhancement: 1500 UTC 17 January 1988: The boundaries of the thresholding area are outlined by the white lines.

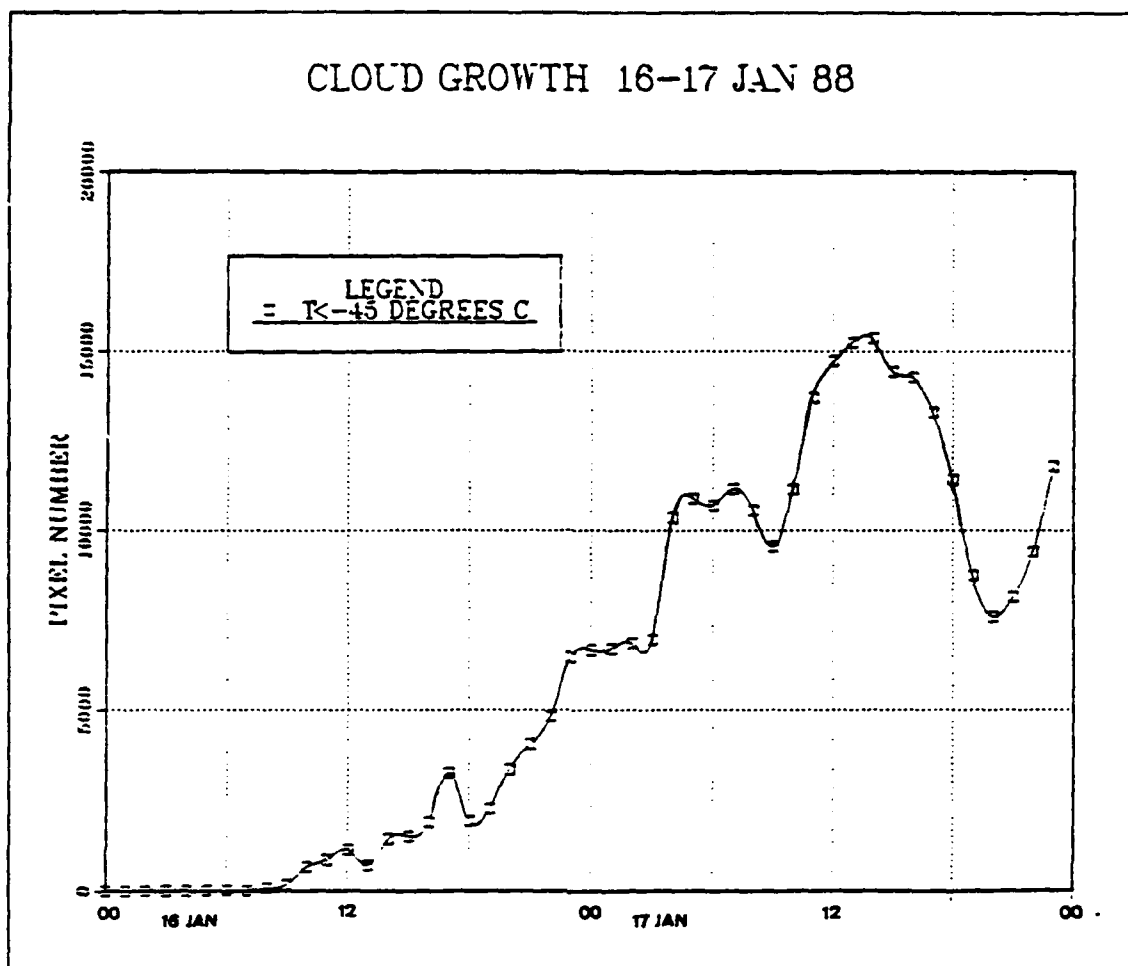


Fig. 9. Cloud growth: 00 UTC 16 January 1988-00 UTC 18 January 1988: This curve represents an expansion of the curve representing a threshold temperature of -45°C .

A correlation coefficient was calculated using the eight central pressure values from the NMC final surface analyses and the corresponding number of pixels colder than -45°C . The correlation coefficient was found to be -0.91 . It is evident for this case that there is a strong negative correlation between the growth of clouds with a temperature threshold of -45°C and the evolution of the central pressure. Although the correlation coefficient utilizes only eight points due to the unavailability of hourly pressure measurements, it does indicate the strong relationship between cyclone development and the coldest cloud tops.

B. CASE 2: 14-16 DECEMBER 1987

1. Overview

The development of this storm occurred in stages similar to those described in Case 1. A detailed analysis of the dynamic and thermodynamic processes leading to the development of this storm is provided by Curtis (1988). Curtis outlined the stages of development as follows:

1. Open wave stage (1200 - 1800 UTC 14 December 1987)
2. Explosive stage (1800 UTC 14 December 1987 - 0000 UTC 16 December 1987)
3. Mature stage (0000 - 1200 UTC 16 December 1987)
4. Decay stage (1200 UTC 16 December 1987 - 1800 UTC 17 December 1987).

These stages are illustrated by the central pressure evolution on Fig. 10.

This storm was of greater intensity than Case 1 and affected a larger area. The open wave stage is characterized by the presence of a comma cloud pattern located near 45° N, 150° W that is visible in the GOES imagery. (Fig. 11). This comma cloud eventually evolves into a head cloud by 0000 UTC 15 December 1987. During the explosive stage the central pressure of the storm dropped 38 mb to a low of 978 mb. In the early phases of the explosive stage the cloud patterns indicate the formation of the Type A cloud pattern (Weldon, 1979) showing a cirrostratus deck or cirrus shield with an anticyclonically-curved northern edge along the west coast of the United States (Fig. 12). By the mature stage, however, the cirrostratus deck becomes wrapped around the circulation center forming spiral vortex more indicative of a Type B pattern.

The movement of the storm is illustrated by the storm track shown in Fig. 13. The storm track is based on the positions of the cyclone obtained from the NMC final surface analyses. Like Case 1, this storm moved primarily in the eastward direction. During the open wave and explosive stages the storm movement paralleled 37° N. After reaching maturity, the storm alters course to the southeast, moving along the California coast until it dissipates.

2. Thresholding Results

The analysis period for this case extends from 1200 UTC 14 December 1987 to 1500 UTC 15 December 1987. This period covers the open wave stage and most of the explosive stage. The end of the coverage is due to the eastern boundary of the satellite data sector which is 120° W longitude. Although the position of the low was west of this boundary for the duration of the development, after 1500 UTC 15 December 1987

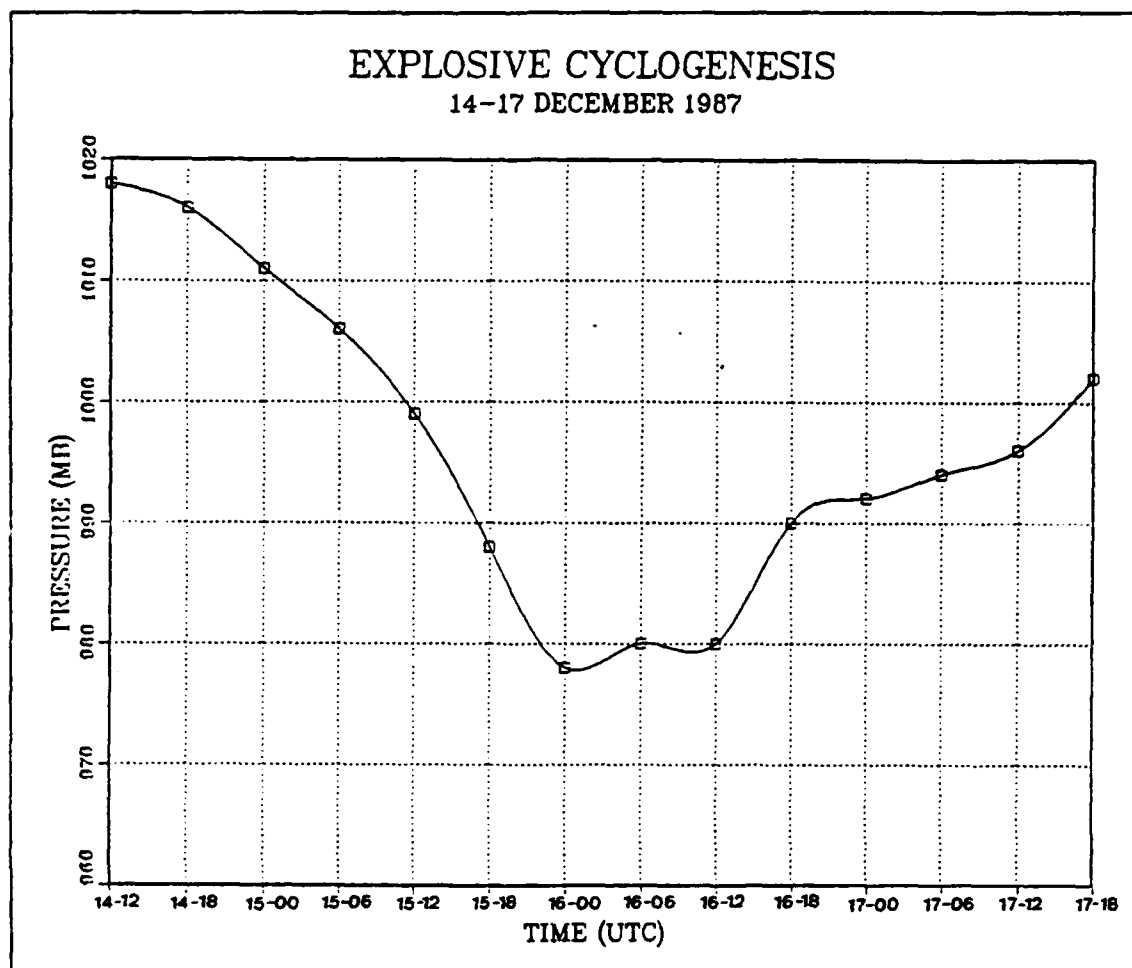


Fig. 10. Central pressure evolution: 14 - 17 December 1987 from Curtis (1988).

the cloud fields of the storm move through this boundary and affect the cloud area computations.

The dimensions of the thresholding area required for this case was 440 pixels by 440 pixels, which is nearly double the area required for Case 1. The dimensions of the thresholding area were established using the 1500 UTC 15 December 1987 image. The boundaries were chosen to ensure that the coldest clouds of the storm's cloud field were enclosed in the thresholding area. The size of the thresholding area was kept constant for all images and are outlined in later figures.

Based on the results of Case 1, the analysis effort was focused on the cloud tops colder than -45°C . The results of the thresholding process for a threshold temperature of -45°C is shown in Fig. 14. As in Case 1, there is a noticeable increase in the number

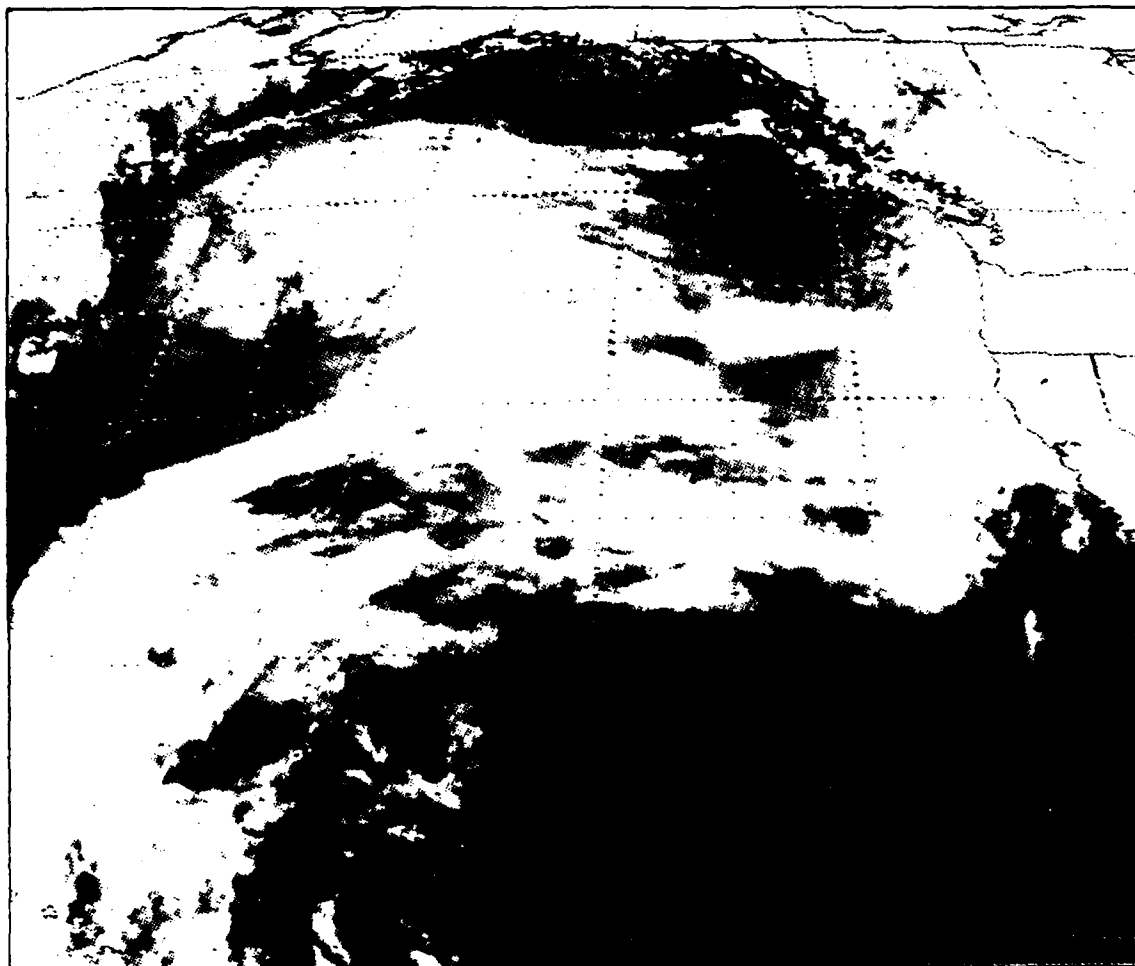


Fig. 11. GOES imagery: 1346 UTC 14 December 1987.

of pixels associated with clouds colder than -45°C during the explosive period. Comparing the cloud growth curve with the central pressure evolution (Fig. 10) reveals a strong negative correlation with the pressure dropping from 1018 mb to 993 mb.

The color enhancement for 1200 UTC 14 December 1987 (Fig. 15), the open wave stage, shows that the thresholding area is dominated by cloud tops colder than -25°C . In the northern half of the thresholding area a pattern resembling a comma cloud can be associated with the 500 mb trough located at 150°W . To the south, a baroclinic zone cloud band dominates. It is in this baroclinic cloud band that the largest area of cloud tops colder than -45° can be found.

By 0000 UTC 15 December 1988 the cloud field of the system, now in the explosive stage, has become more compact and has formed a solid head cloud (Fig. 16).

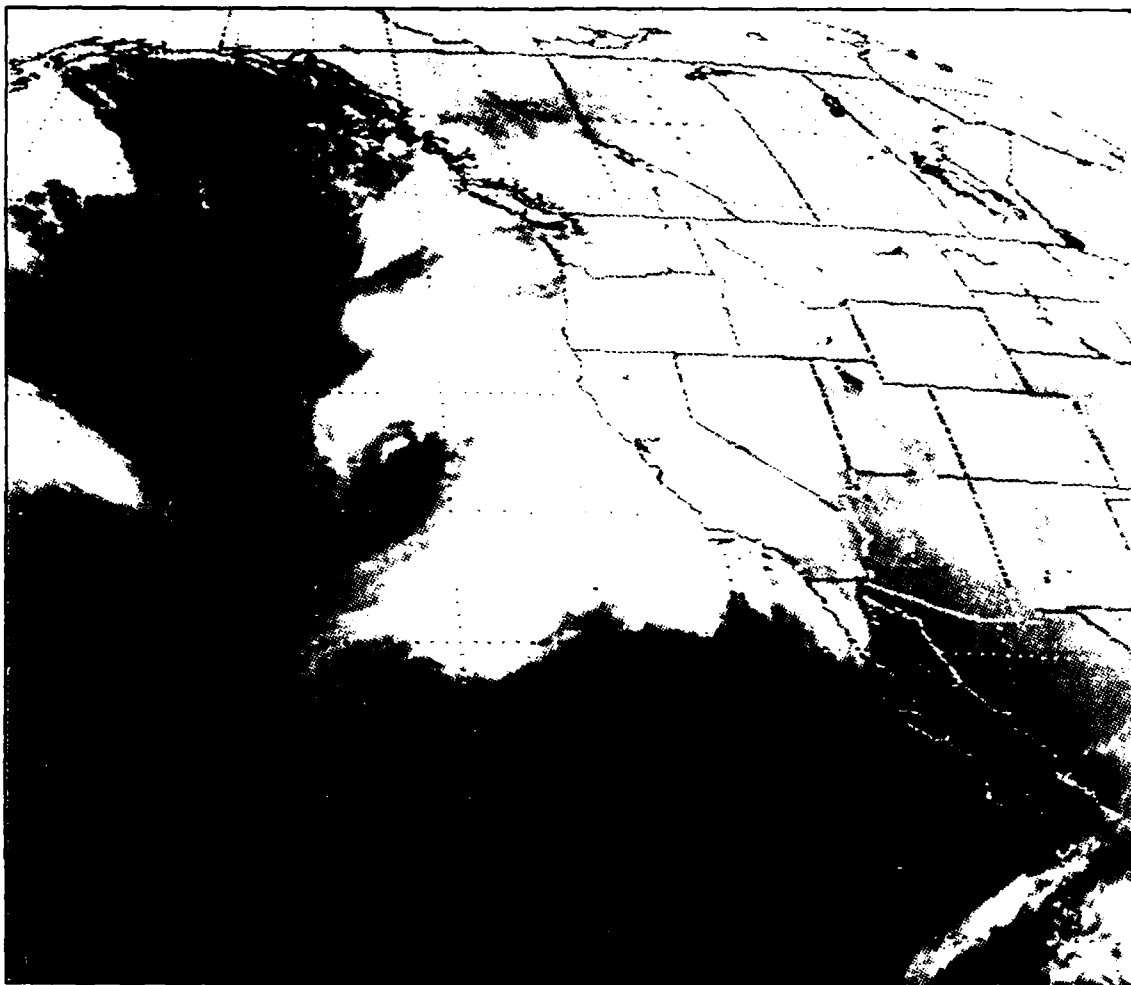


Fig. 12. GOES imagery: 1546 UTC 15 December 1987.

This head cloud is composed primarily of cloud tops colder than -35°C with a large concentration of cloud tops colder than -45°C at the center of the head cloud. The size of the area associated with the -45° threshold is now nearly twice the size shown in Fig. 15. A significant area of cloud tops colder than -55°C is also visible. The sharp anticyclonically-curved northern boundary of the head cloud is well defined by cloud tops colder than -35°C .

As the storm deepens, the growth of clouds colder than -45°C appears in two primary locations (Fig. 17). The largest concentration of these cloud tops are in the storm's cirrostratus deck or cirrus shield. This cirrus shield develops to the east of the storm's center and appears as a massive canopy over the comma cloud. In this cirrus

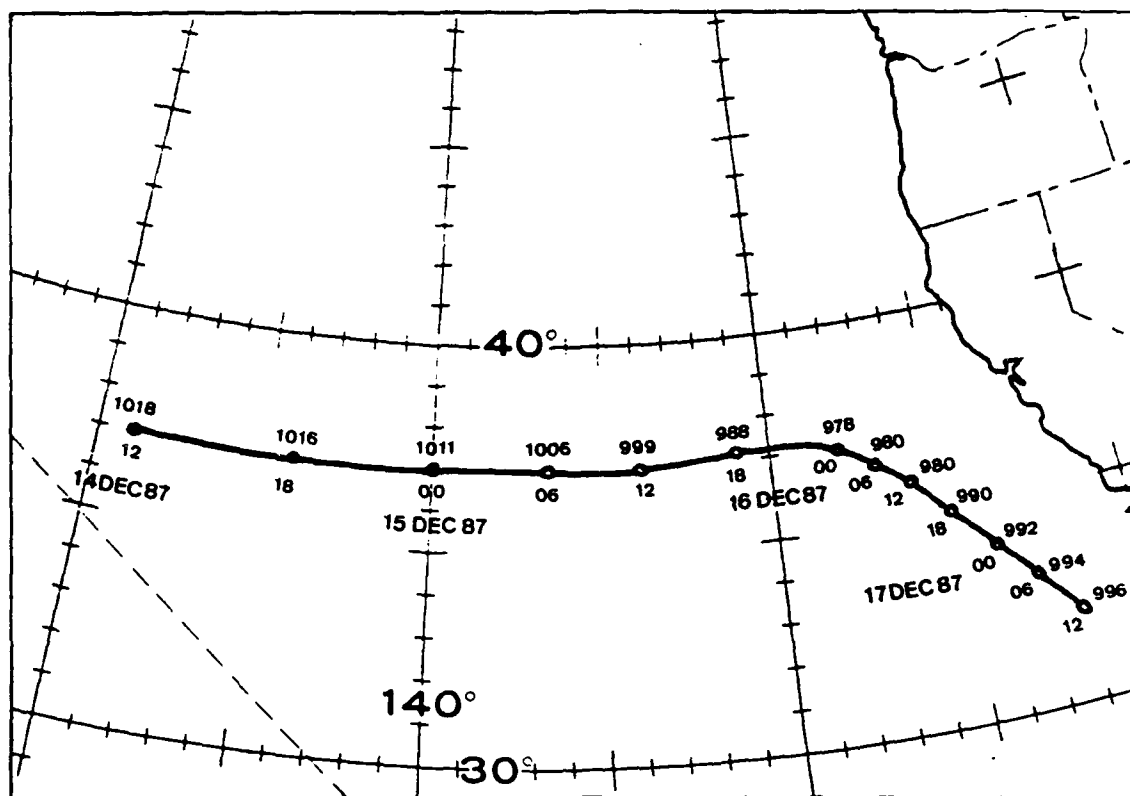


Fig. 13. Storm track: 14 - 17 December 1988.

shield there are also significant areas of clouds colder than -55°C with some of these clouds being less than -60°C . The second location is directly to the northeast of the storm center above the occlusion area. The size of the area covered by clouds colder than -45°C is now approximately four times the size at the start of the analysis period.

Although it was not possible to carry out the thresholding process to the mature stage the results indicate that as the storm deepened a noticeable increase in cloud area was observed. As in Case 1, the increase in cloud area is most evident for cloud top temperatures colder than -45°C . However, the location of the -45°C cloud tops differed greatly. While cloud growth for Case 1 was concentrated over the occlusion area, for this case cloud tops of -45°C threshold temperatures were found primarily in the large cirrus shield located to the east of the storm center with only a small concentration located at the head of the comma cloud.

Analysis of imagery enhancements from 1500 UTC 15 December 1987 thru 0000 UTC 16 December 1987 indicates another difference from Case 1. In Case 1, the

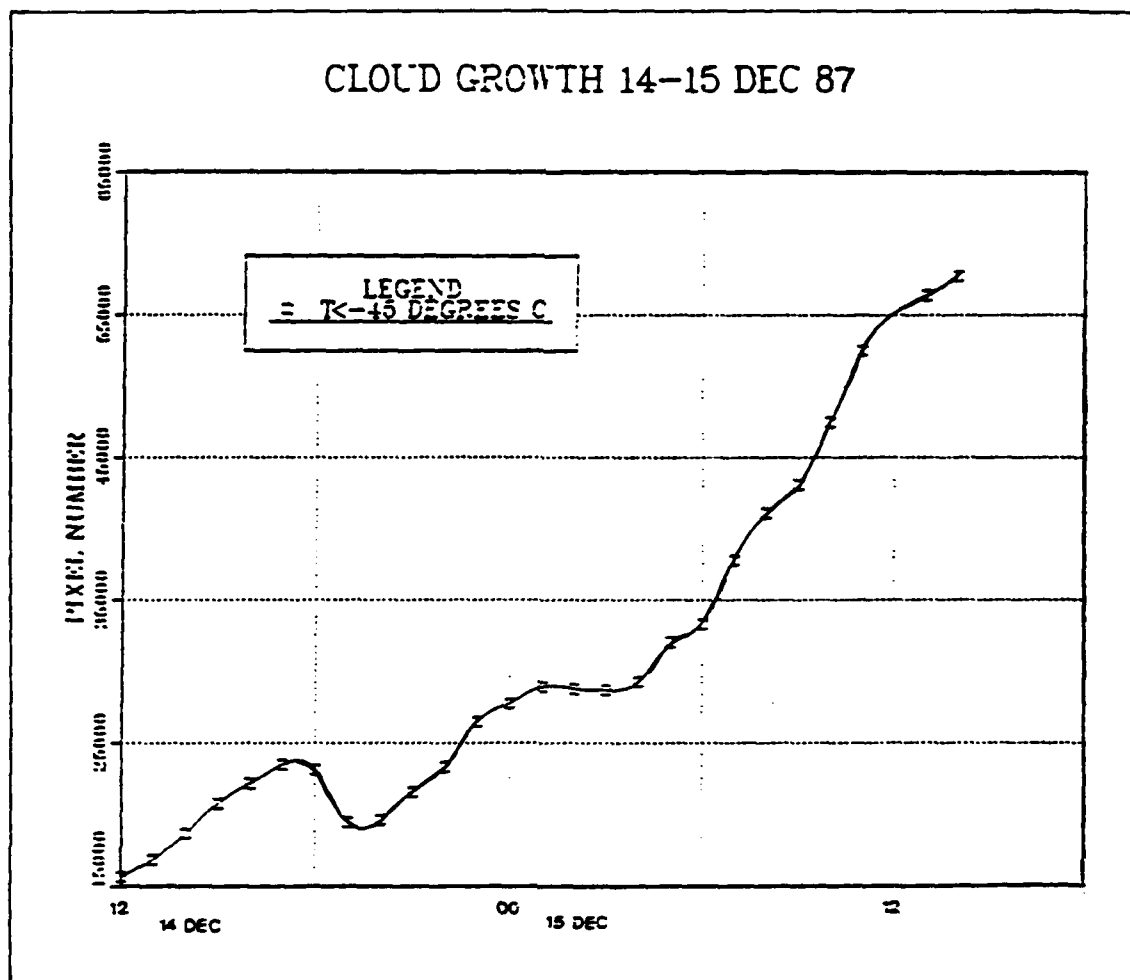


Fig. 14. Cloud growth: 14 - 15 December 1987.

maximum areal coverage of clouds colder than -45°C occurred at the same time the storm reached its deepest central pressure. For this case, a comparison of imagery of the storm at its deepest central pressure (Fig. 18) with the imagery for 1500 UTC 15 December 1987 (Fig. 17) indicates a significant reduction of the clouds colder than -45°C near the center of the cyclone. Fig. 18 also shows a pattern without the cirrus shield shown in the earlier phase of the explosive stage and clouds colder than -45°C concentrated primarily over the occlusion region.

The correlation coefficient for the cloud growth curve and the central pressure curve for the analysis period is -0.98 . This indicates a nearly perfect inverse correlation. However, the image enhancements for times after the analysis period indicate that the

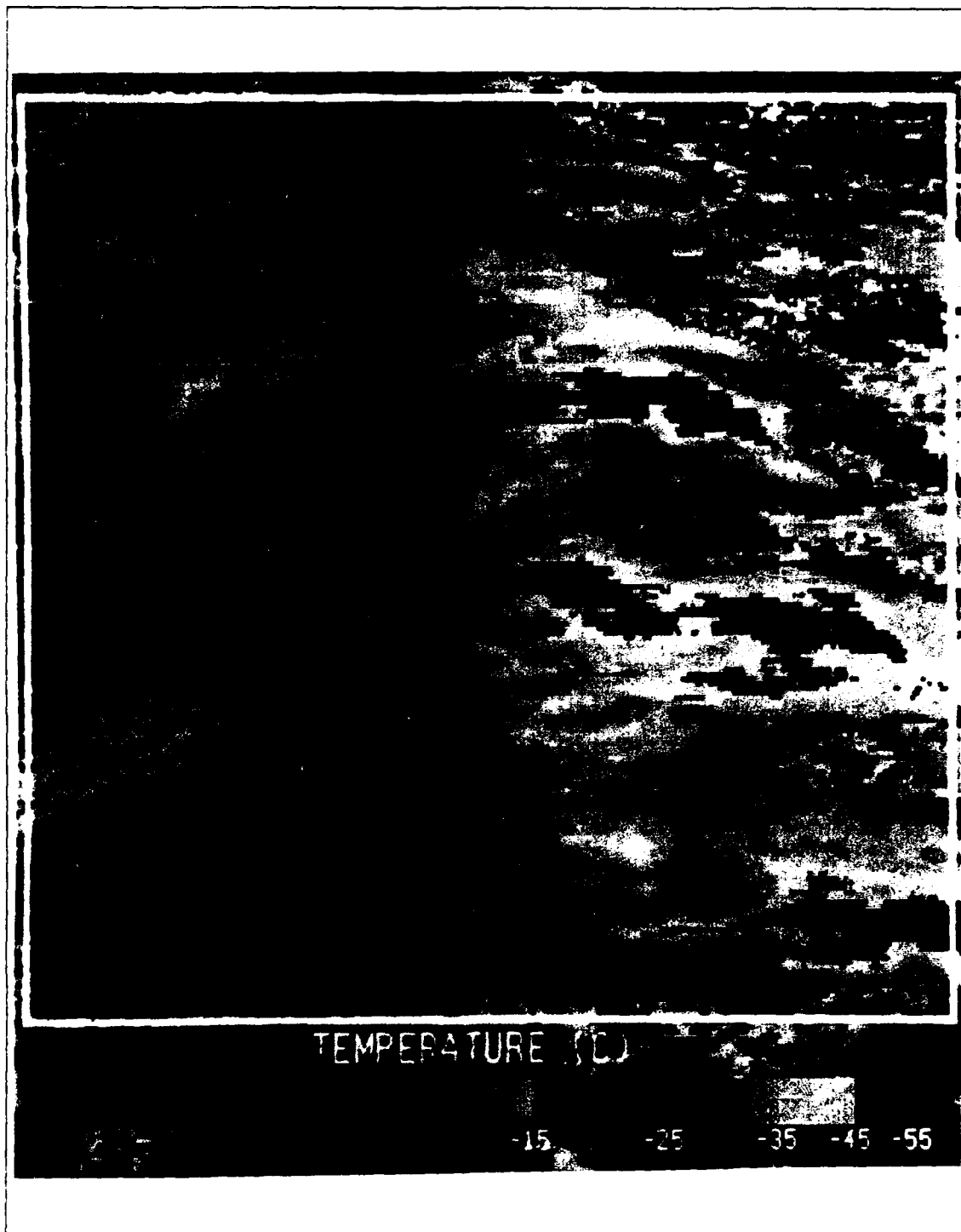


Fig. 15. IR image enhancement:1200 UTC 14 December 1987.

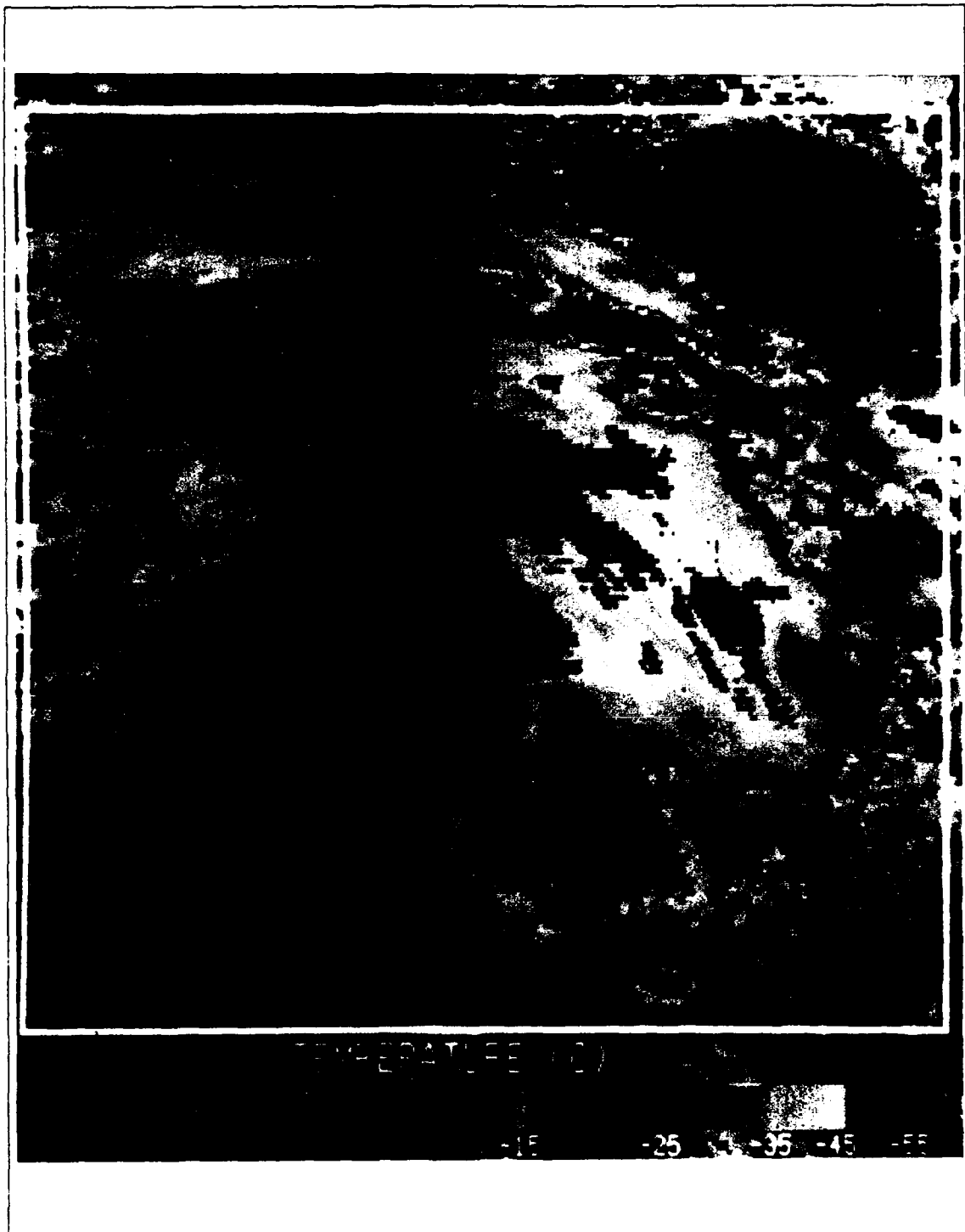


Fig. 16. IR image enhancement:0000 UTC 15 December 1987.



Fig. 17. IR image enhancement:1500 UTC 15 December 1987.



Fig. 18. IR image enhancement:0000 UTC 16 December 1987.

number of pixels actually decreases as the pressure continues to drop. This implies that if the thresholding process was continued up to the mature stage of development, the correlation would probably not be as strong. Case 2, while differing in the type of cyclone cloud pattern, does show the same correlation of the cold cloud tops with rapid cyclogenesis. However, the correlation was strongest during the first half of the rapid deepening period.

C. CASE 3: 1 - 2 JUNE 1988

1. Overview

The development of this storm followed the same stages noted in Case 1 and 2. The evolution of the central pressure during the analysis period is shown in Fig. 19. The analysis period for this storm extends from 1800 UTC 1 June 1988 thru 2000 UTC 2 June 1988. This period extends from the latter phase of the open wave stage when a baroclinic leaf pattern appears in the GOES-West imagery (Fig. 20) to the storm's maturity when it reached a central pressure of 968 mb.

The cloud patterns of this storm during the explosive stage were similar to the patterns shown by Case 2. In the early phase of the explosive stage the baroclinic leaf evolves to a Type A pattern described by Weldon (1979). The cirrostratus deck overlying a comma cloud that characterize the Type A pattern are clearly visible in the imagery shown in Fig. 21.

The movement of the storm is shown in Fig. 22. Throughout the open wave stage the storm moved to the east along 39° N. At the beginning of the explosive period the storm changes course to the northeast and remains on this course until it reaches the mature stage at 48° N, 131° W. Once mature, the storm moves north along the coast until it dissipates.

2. Thresholding Results

There are two major factors not present in the previous cases that must be considered for this case. The first is that the resolution of the PC MCIDAS data is lower than the full resolution data used in the first two cases and may not reflect some of the small changes in cloud structure previously seen. The second is the movement of the storm during the analysis period. Glover (1974) found that the ground spatial resolution of a geostationary satellite image degrades with distance away from the satellite subpoint due to the curvature of the earth. He also noted that the resolution degrades rapidly beyond a 42° arc from the satellite subpoint. For the first two cases, the predominantly eastern movement of the storms was within the 42° arc and the satellite resolution was approximately 1.5 times the resolution at the satellite subpoint for the entire analysis period. Because there was virtually no change in the satellite resolution, the number of pixels provided an accurate representation of the areal coverage. For this case, the movement of the storm carried it beyond the 42° arc resulting in a change of resolution from 1.5 times to about 2.0 times the resolution at the satellite subpoint during the analysis period. This represents a significant degradation in resolution that introduces inaccuracies in the use of the number of pixels to represent cloud areal coverage.

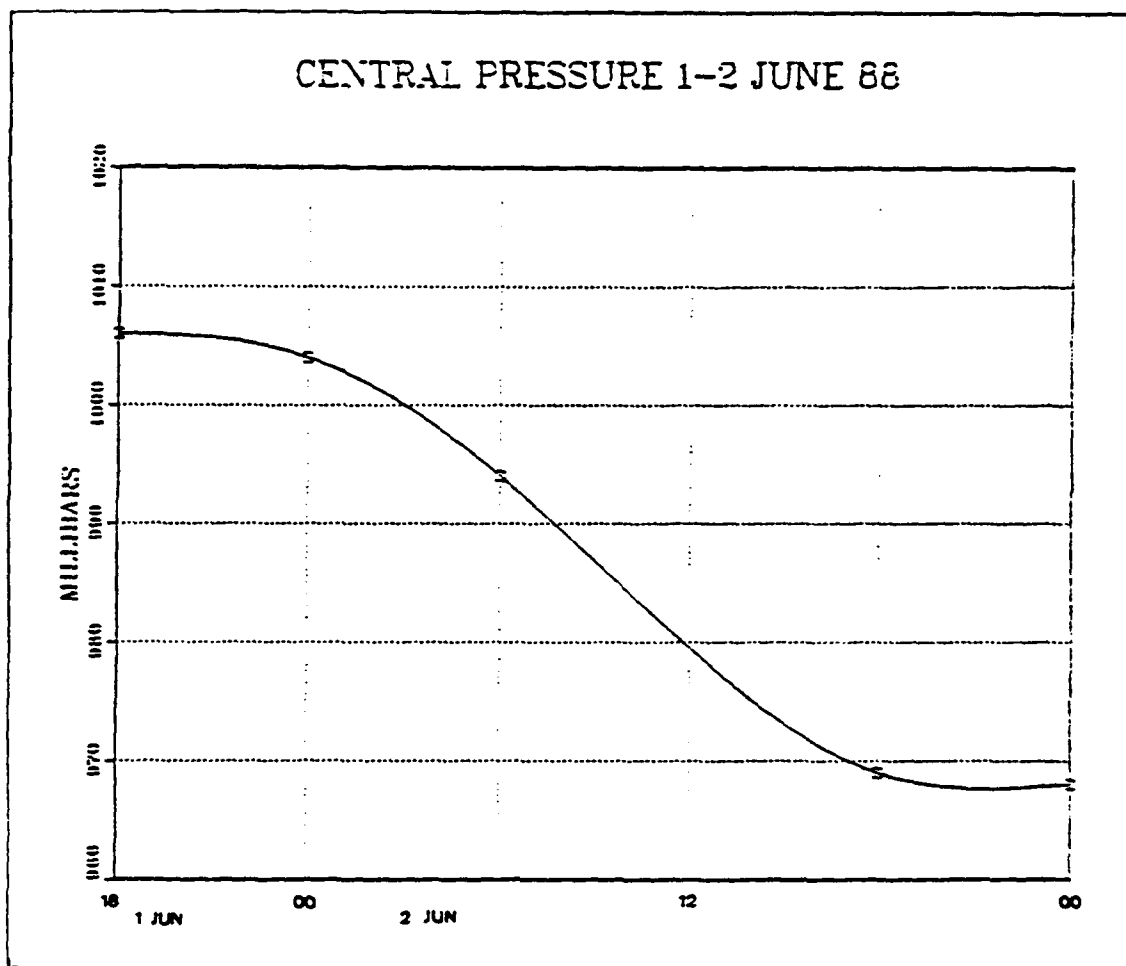


Fig. 19. Central pressure evolution: 1 - 2 June 1988.

However, even with these inaccuracies, it is still possible to use the increase in the number of pixels to represent cloud growth trends since an increase in pixels still indicates an increase in cloud area.

As in the first two cases, the analysis of this storm focused on the growth of cloud tops colder than -45°C . Although the cloud fields of this storm covered approximately the same amount of area as Case 1, the number of pixels counted were considerably less due to the lower resolution of the PC MCIDAS data. While the average number of pixels for a threshold temperature of -45°C for Case 1 was 8232 pixels, the average number for this case was 1323 pixels. The results of the thresholding process are presented in Fig. 23. The size of the thresholding area for this case was kept constant at 150 pixels by 200 pixels.

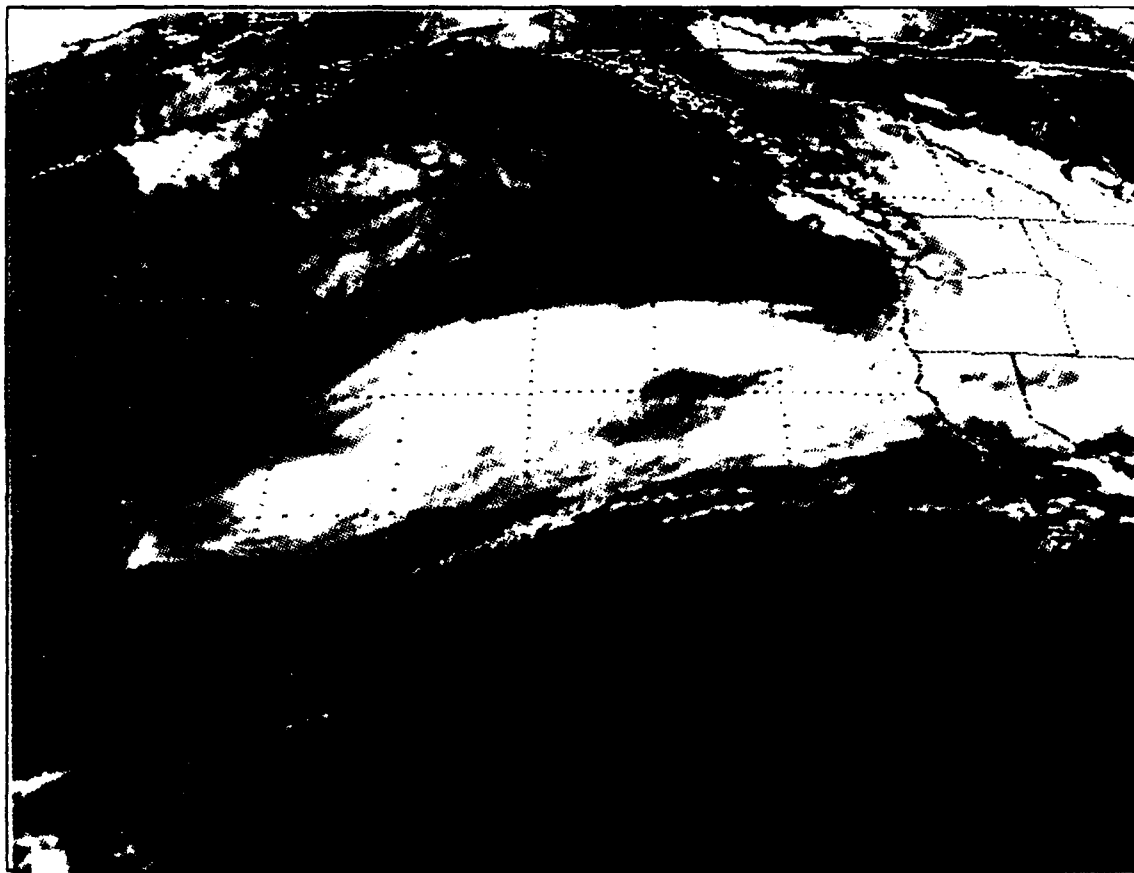


Fig. 20. GOES imagery: 1746 UTC 1 June 1988.

The early stage of the analysis period is characterized by a steady increase in the number of pixels colder than -45°C . This increase occurs in the latter phase of the open wave stage of development and continues into the early phase of the explosive stage. By 0500 UTC 2 June 1988 a maximum number of 2239 pixels is reached and followed by a dramatic decrease to 1138 pixels by 0700 UTC. The decrease in number of pixels continues for the next three hours reaching a minimum of 823 pixels before increasing steadily again for the remainder of the analysis period.

The image enhancements (Fig. 24 - Fig. 27) show that the noticeable changes in cloud structure are in fact most visible for threshold temperatures of -45°C . The 1800 UTC 1 June 1988 enhancement (Fig. 24) shows that the cloud tops colder than -45°C are concentrated primarily in two regions. The larger of the two regions lies near the northern edge of the cloud mass along the jet axis. To the south is a much smaller

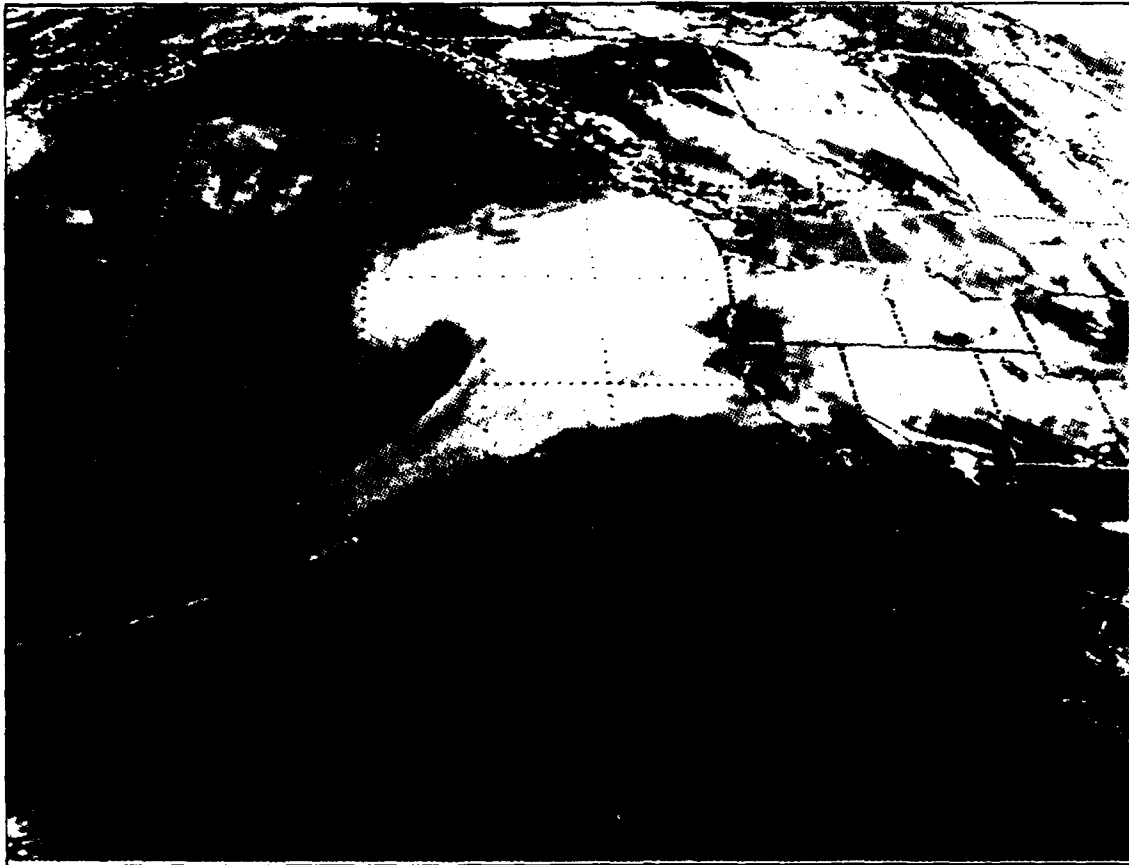


Fig. 21. GOES imagery: 0546 UTC 2 June 1988.

wedge-shaped region. The total number of pixels for a temperature threshold of -45°C is 1103 pixels.

By 0300 UTC 2 June 1988, a cirrostratus deck or cirrus shield and a comma cloud can be seen in the image enhancement (Fig. 25). The -45°C cloud tops are found in two large areas in the cirrus shield. Fig. 25 shows that both of these areas are found near the trailing edge of the cirrus shield and that the much of the growth takes place around the small wedge-shaped region shown in Fig. 24. The area with cloud tops colder than -45°C also exhibits some growth and appears to become more compact. By this time the number of pixels has increased to 1813.

The 1200 UTC 2 June 1988 enhancement (Fig. 26) shows a significant reduction in cloud tops colder than -45°C . Only 883 pixels remain and much of this is concentrated near the western edge of the cirrus shield. However, unlike the previous

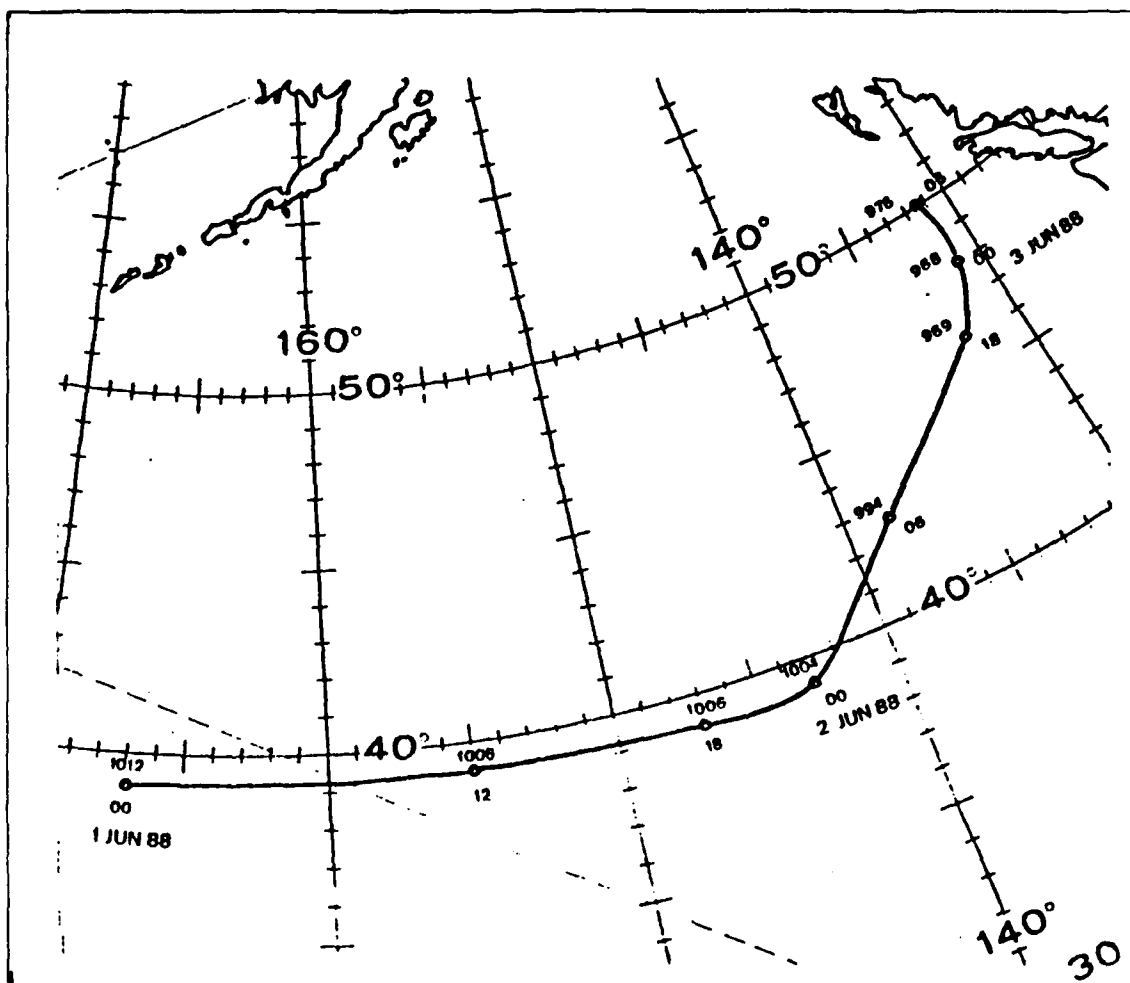


Fig. 22. Storm track: 1 - 3 June 1988.

enhancements, some of these cloud tops appear in the comma cloud. The cirrus shield appears much smaller than before and now extends to the north of the storm center.

By 2000 UTC 2 June 1988 the storm has reached maturity and has formed a Type A pattern (Fig. 27). A large portion of the cirrus shield overlies the fully developed comma cloud and the western edge of the shield is well defined. Once again the cloud tops colder than -45°C are concentrated in the cirrus shield and have increased in number to 2055 pixels.

A correlation coefficient was calculated using the five central pressures obtained from available analyses and the number of pixels counted for the same time. The result of the calculation was a correlation coefficient of -0.24 . This implies a small negative

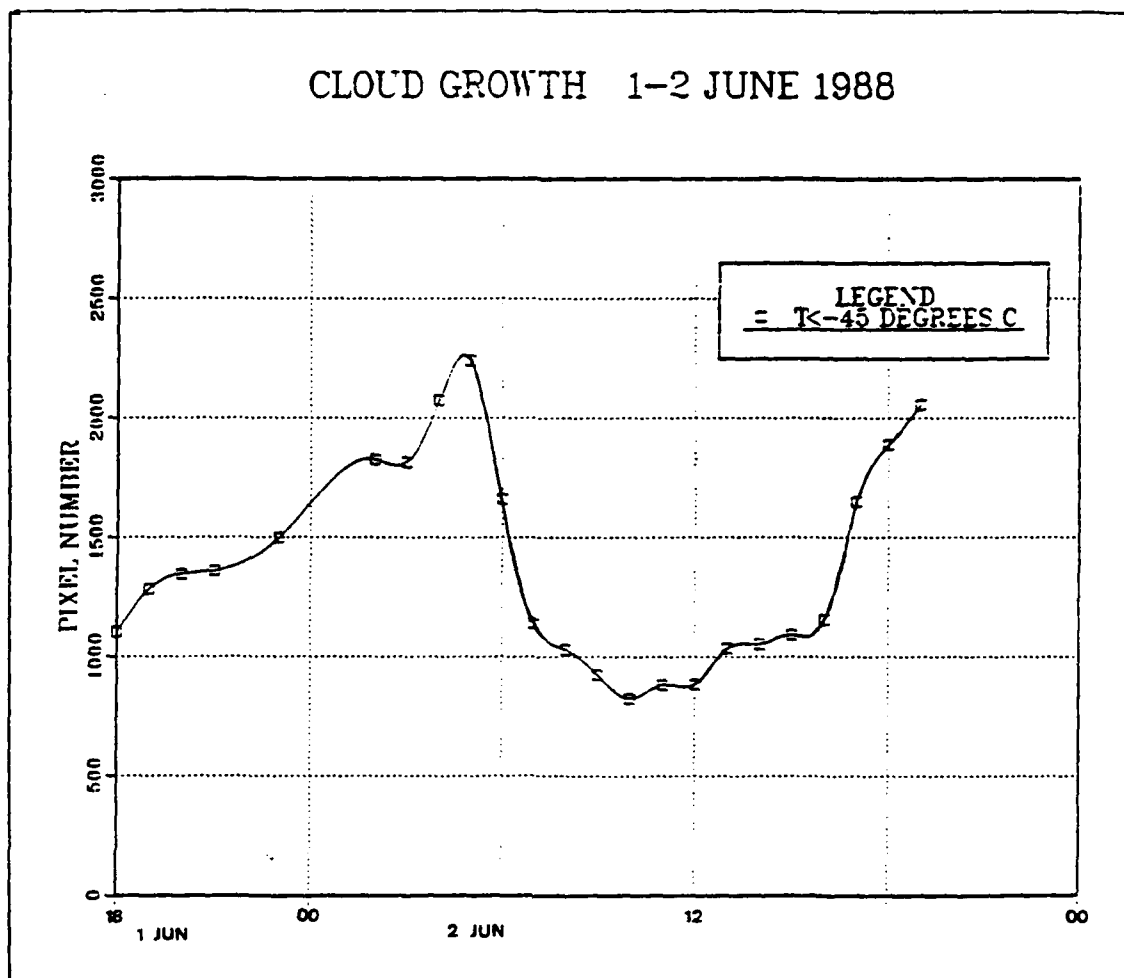


Fig. 23. Cloud growth: 1 - 2 June 1988.

correlation between pressure deepening and cloud growth. However, this is not an accurate measure because the number of pixels themselves do not provide an accurate measure of cloud growth due to the lower resolution of the data and the further degradation of this resolution by the northward movement of the storm. If one accounts for the larger pixel areas (due to the rapid northeastward movement), the area of the coldest cloud tops would show overall growth and considerably higher correlations. This area computation is required in order to properly interpret storms with significant meridional displacements.

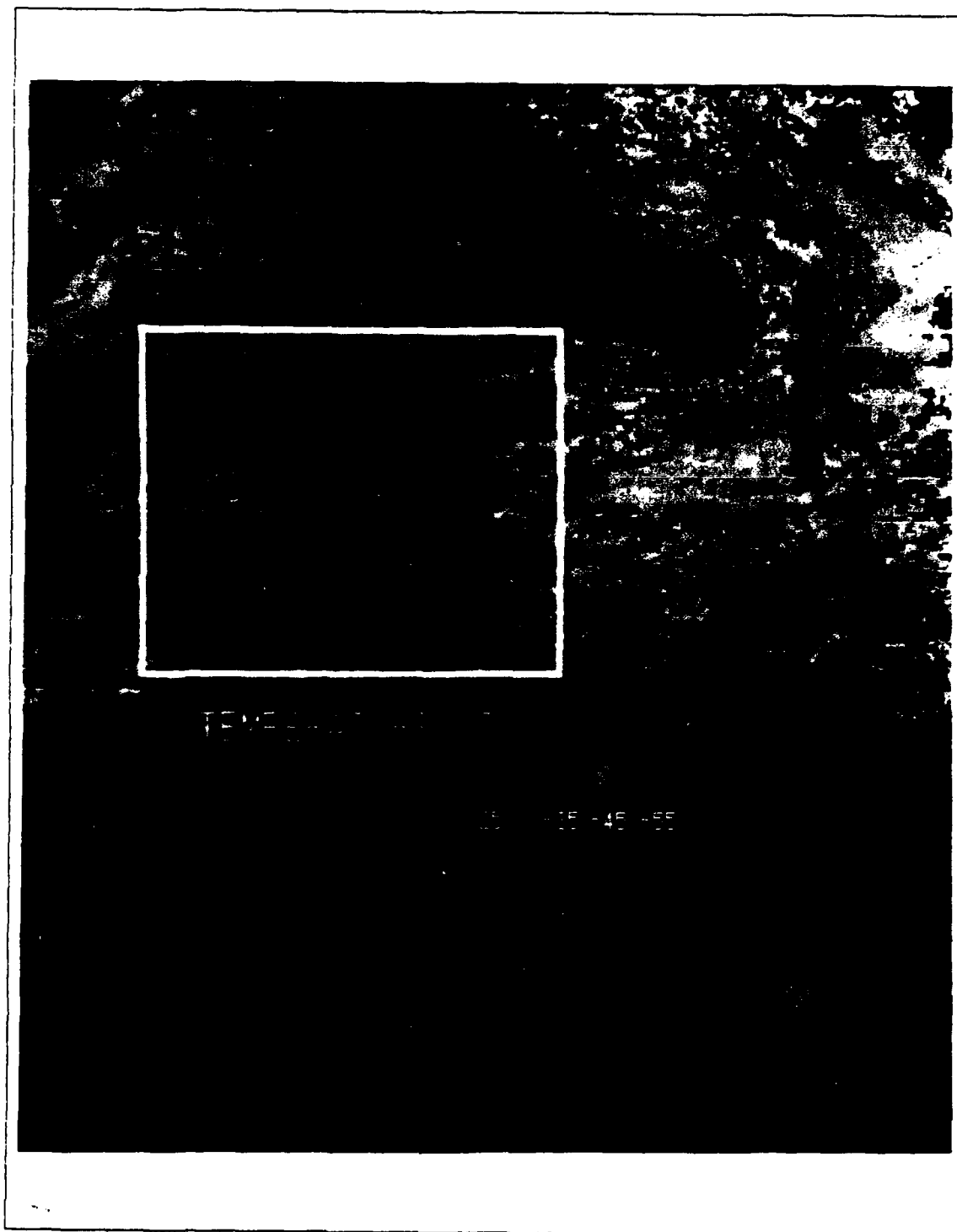


Fig. 24. IR image enhancement:1800 UTC 1 June 1988.

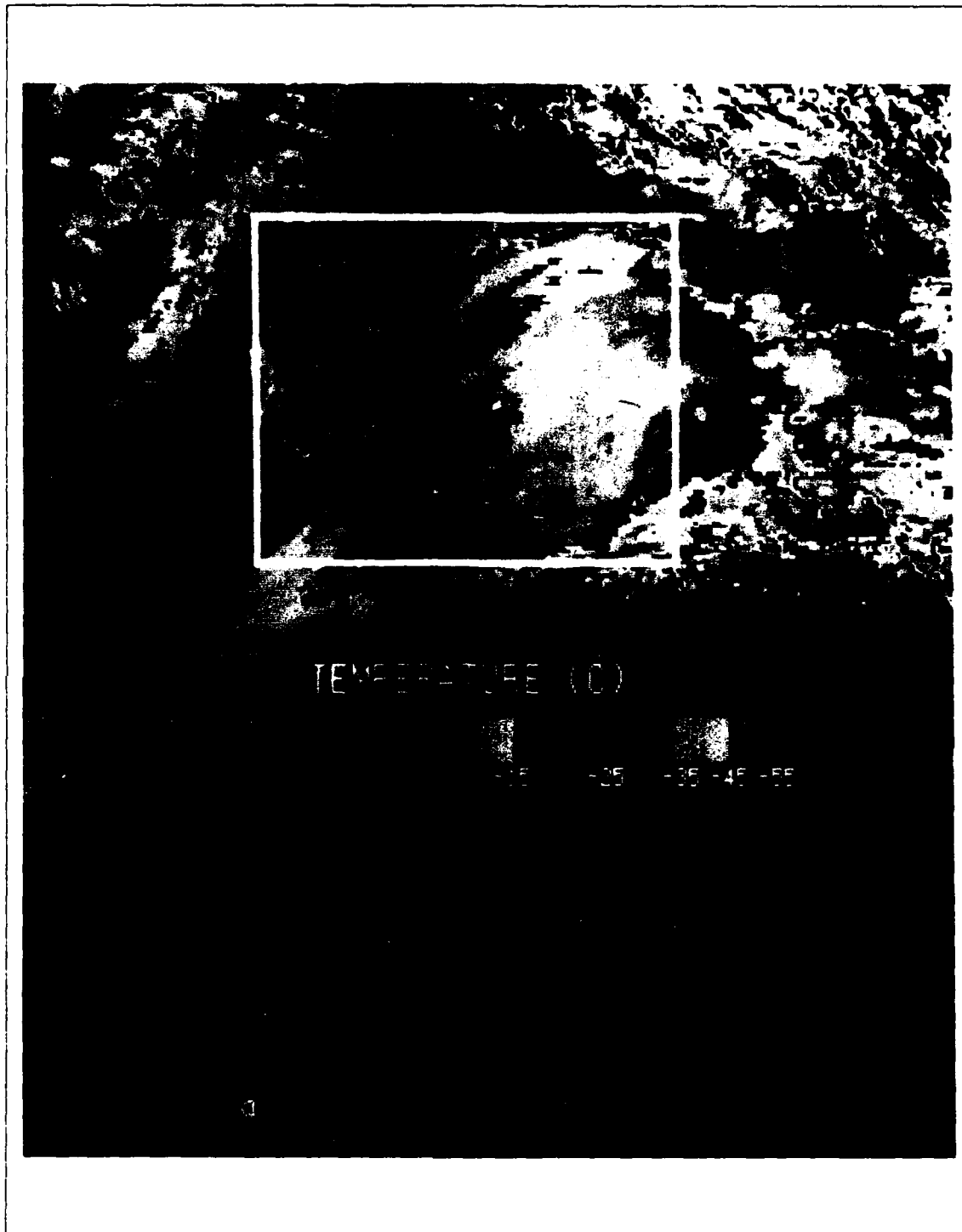


Fig. 25. IR image enhancement:0300 UTC 2 June 1988.

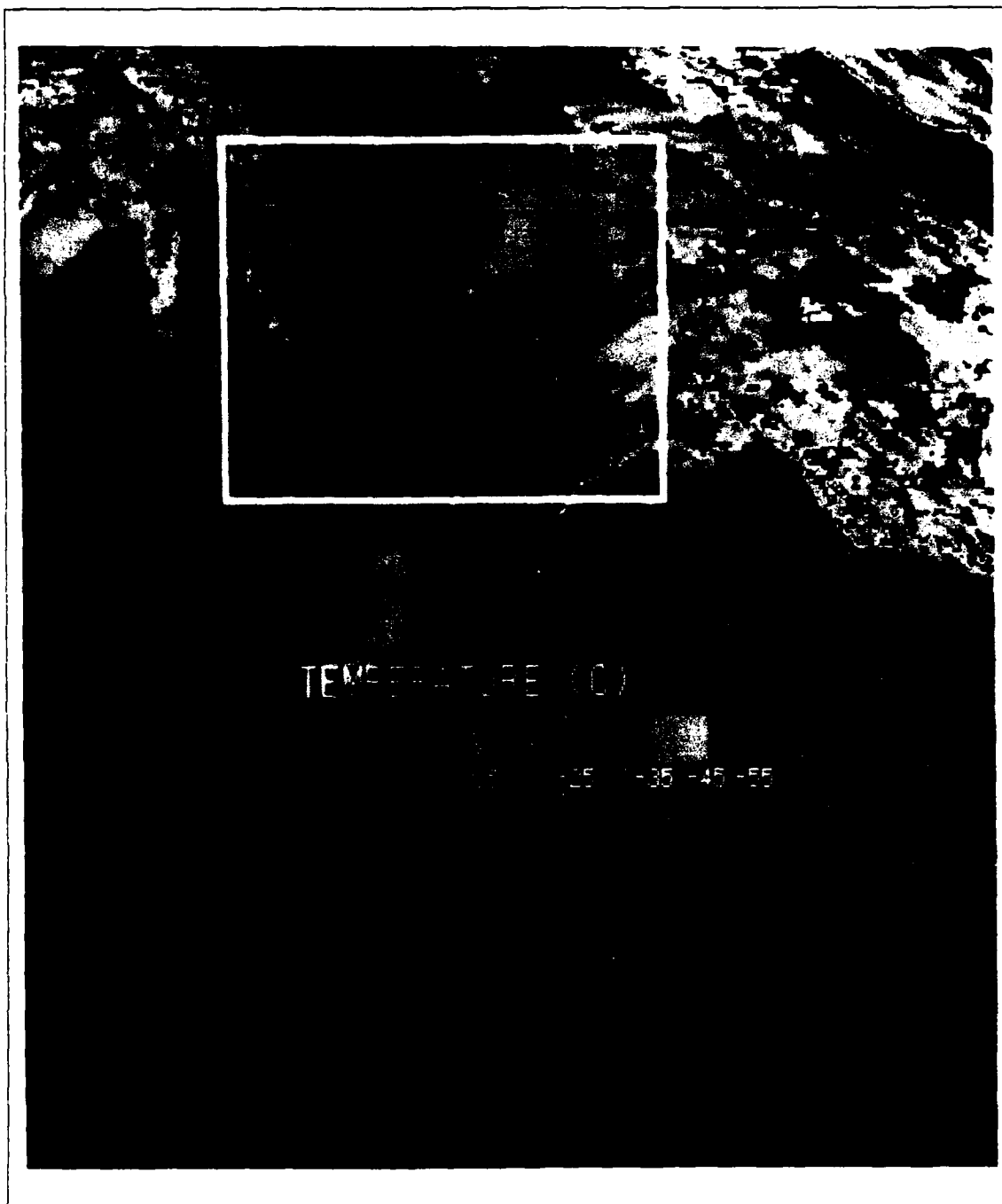


Fig. 26. IR image enhancement: 1200 UTC 2 June 1988.

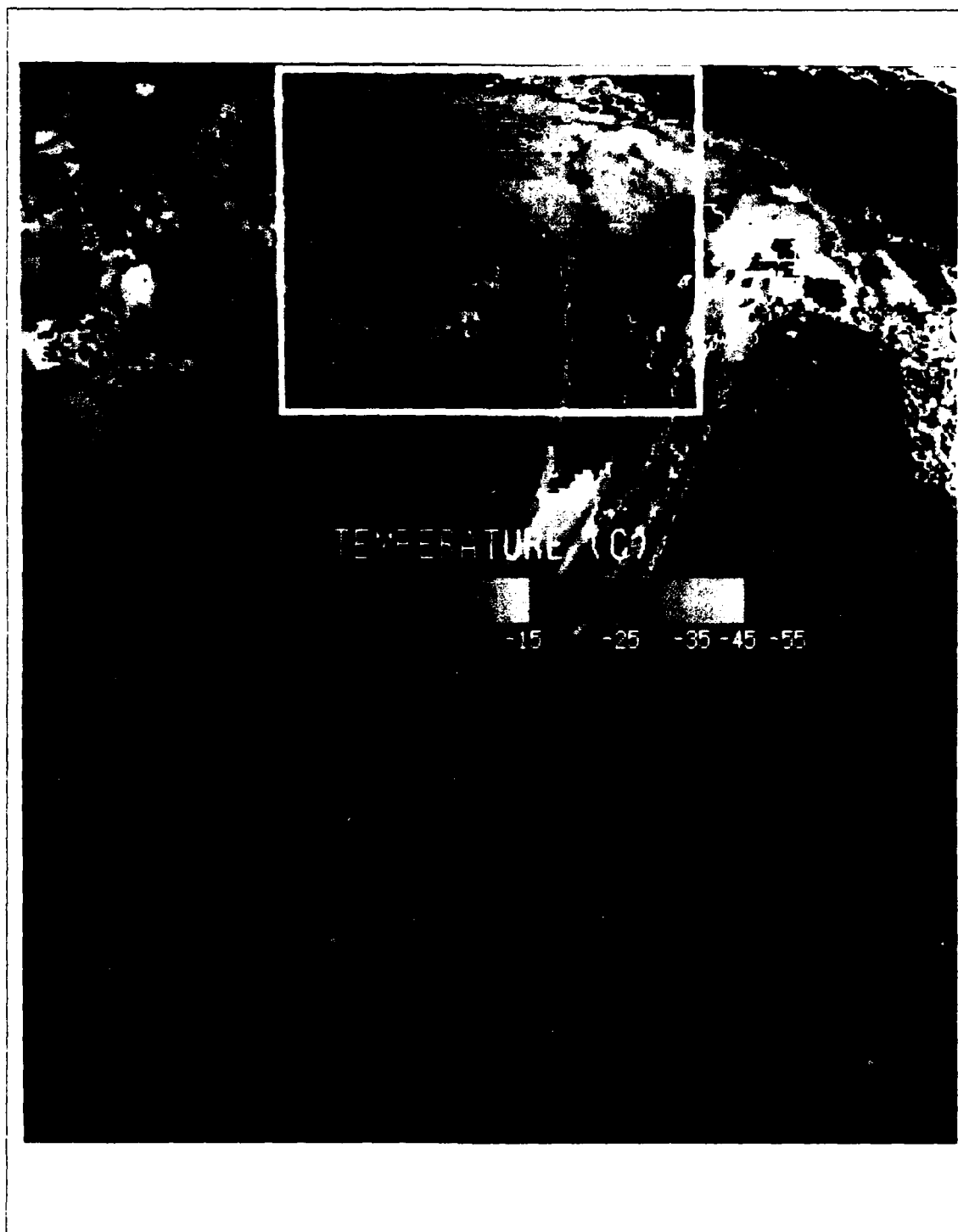


Fig. 27. IR image enhancement:2000 UTC 2 June 1988.

D. SUMMARY

Animation of visual and infrared imagery has indicated that rapid cloud growth is a characteristic of explosively-developing cyclones. The working hypothesis in this thesis is that the intense vertical motions responsible for the low-level spin-up will produce rapid cloud expansion in the upper troposphere that can be detected using digital satellite data. Applying this hypothesis, the cloud growth of three explosive storms that developed over the eastern North Pacific Ocean was examined using a thresholding process to determine the cloud area coverage.

The results of Case 1 indicate that the increase in area of the coldest cloud tops are most closely related to the rapid development period. For a threshold of -45°C the most rapid increase in cloud area occurred during the explosive stage of development. The maximum extent of the areal coverage of cloud tops colder than -45°C was attained when the storm reached its deepest pressure. For cloud tops warmer than -45°C much of the cloud growth occurred during the open wave stage. The image enhancements show that at its mature stage the storm had a Type B pattern described by Weldon (1979) and the coldest clouds were concentrated over the occlusion region.

During the explosive stage of Case 1, the central pressure dropped 21 mb while the number of pixels increased from 1935 to over 15000. This indicates a strong negative correlation between pressure deepening and cloud growth. The correlation was calculated as -0.91 .

As in Case 1, the results of Case 2 indicate that the growth of cloud tops colder than -45°C is closely related to the deepening of the central pressure. During the analysis period, the central pressure decreased from 1018 mb to 993 mb while the number of pixels for a threshold temperature of -45°C increased from 15674 pixels to over 58000 pixels. The image enhancements for this period show a Type A cloud pattern described by Weldon, which is characterized a large cirrus shield or cirrostratus deck overlying a maturing comma cloud. The largest concentration of cloud tops colder than -45°C were located in the cirrus shield with a smaller group appearing over the occlusion area of the comma cloud. A correlation of -0.98 was calculated for the analysis period indicating a very strong relationship between pressure deepening and cloud growth. However, this correlation does not include the 9 h period preceding the storm's maturity. Image enhancements of this 9 h period indicate that the maximum extent of cloud growth may have been reached prior to the storm's maturity. This implies that the actual correlation is probably less.

The Case 3 storm analysis used the PC MCIDAS data which is of lower resolution than data used for the first two cases. There is also a rapid decrease of the data resolution resulting from the storm's northward movement. These inaccuracies limit the effectiveness of using the number of pixels to represent the cloud area coverage. It was still possible to relate the increase in the number of pixels to the increase in cloud area; however, the amount of growth was not accurately determined.

The results of Case 3 indicate a steady increase in the number of pixels with a temperature threshold of -45°C until 0500 UTC 2 June 1988. This increase was immediately followed by a dramatic reduction in pixels from 2239 to 823 pixels before increasing once again. The correlation between pressure deepening and area change was calculated at $-.24$, indicating weak correlation. Like Case 2, the image enhancements for this storm show a Type A pattern with the largest concentration of clouds colder than -45°C located in the cirrus shield. The maximum extent of the cloud area coverage was attained nearly 15 h prior to the storm reaching its deepest pressure.

V. CONCLUSIONS AND RECOMMENDATIONS

The objectives of this thesis were to demonstrate the feasibility of using digitized satellite data to analyze quantitatively the cloud structure of explosive cyclones and to study the relationship between pressure deepening and cloud growth. The results of the case studies indicate that the growth in areal coverage of clouds colder than -45°C is most closely related to the explosive development period. However, this relationship is dependent on the cloud pattern of the maturing cyclone.

For a Type A cloud pattern, which is characterized by a cirrus shield overlying a comma cloud, the results indicate that the maximum extent of cloud areal coverage for clouds colder than -45°C is reached prior to the storm's maturity. These clouds appear to be concentrated primarily in the cirrus shield with a smaller concentration sometimes found in the comma cloud. In contrast, for a Type B pattern, which does not have the cirrus shield, the maximum extent of cloud coverage for clouds with a temperature threshold of -45°C was reached at the same time the storm reached its deepest pressure and concentrated primarily over the occlusion area.

It is apparent that digitized satellite data can be used for quantitative analysis of cloud structure. However, the technique used in this study provides only an estimate of cloud growth because it does not account for changes in resolution due to latitudinal and longitudinal changes. For Case 1 and Case 2, the movement of the storms resulted in negligible changes in resolution so the number of pixels was representative of the areal coverage. For Case 3, an accurate estimate of cloud growth could not be obtained due to the degradation of resolution resulting from the storm's northward track.

The correlation coefficients calculated for Case 1 and Case 2 showed a strong negative correlation of $-.91$ and $-.98$, respectively, while Case 3 showed only a $-.24$ correlation. While these correlations indicate that the cloud growth is related to pressure deepening, it must be considered that the calculations were based on pressures and number of pixels at hourly intervals. Therefore, the correlations provides only a general estimate of the relationship between the two parameters. Additionally, this technique does not account for large variations in the amount of convection associated with each storm type.

This study demonstrates the feasibility of using digitized satellite data to quantitatively analyze the cloud growth and structure of explosively developing cyclones.

However, the results of this study do not provide a definitive relationship between pressure deepening and cloud growth. It is clear that further studies of cloud growth, structure and pattern, using digitized data, must be considered.

Recommendations for future studies involving quantitative analysis of digitized satellite data are:

- Incorporate a means of accurately determining the areal coverage of cloud masses by calculating the resolution of each pixel based on position in the thresholding process. The result would be cloud growth measurements based on actual changes in area instead of number of pixels.
- Compare the cloud structure and growth of explosive cyclones with normally developing cyclones and with explosive cyclones of various types.
- Compare the cloud growth and structure measured using digitized data from geostationary satellites with measurements using data from polar orbiting satellites.
- Conduct a statistical study of the cloud growth of explosive cyclones from the open wave stage through dissipation and, from this study, develop a composite to be used as a standard for comparative studies.
- Further document the cloud growth associated with Weldon's Type A pattern with that of a Type B pattern. The quantitative cloud top analysis may be dependent on the type of cyclone cloud band.

Continuing studies hopefully will develop additional methods to use satellite data for quantitative analyses of maritime cyclones.

LIST OF REFERENCES

- Anderson, R.K., J.P. Ashman, G.R. Farr, E.W. Ferguson, G.N. Isayeva, V.J. Oliver, F.P. Parmenter, T.P. Popova, R.W. Skidmore, A.H. Smith, and N.F. Veltischev, 1973: The use of satellite pictures in weather analysis and forecasting, *WMO Technical Note No. 124*, Geneva, Switzerland, 154-161.
- Anthes, R.A., Y.H. Kuo and J.R. Gyakum, 1983: Numerical simulations of a case of explosive marine cyclogenesis. *Mon. Wea. Rev.*, **111**, 1174-1188.
- Bosart, L.F., 1981: The Presidents' Day Snowstorm of 18-19 February 1979: A subsynoptic-scale event. *Mon. Wea. Rev.*, **109**, 1542-1566.
- Bottger, H., M. Eckardt and U. Katergiannakis, 1975: Forecasting extratropical cyclones with hurricane intensity using satellite information. *J. Appl. Meteor.*, **14**, 1259-1265.
- Burfeind, C.R. and J.A. Weiman, 1987: A preliminary computer pattern analysis of satellite images of mature extratropical cyclones. *Mon. Wea. Rev.*, **115**, 556-563.
- Burt, S.D. and D.A. Mansfield, 1988: The great storm of 15-16 October 1987. *Weather*, **43**, No. 3, 90-108.
- Burt, T.G. and N.W. Junker, 1976: A typical rapidly developing cyclone as viewed in SMS-II imagery. *Mon. Wea. Rev.*, **104**, 489-490.
- Curtis, J., 1988: A case study of explosive cyclogenesis in the eastern Pacific Ocean 14-17 December 1987. M.S. Thesis, Naval Postgraduate School, Monterey, Ca., 43 pp.
- Fett, R.W. and W.A. Bohan, 1981: Navy Tactical Applications Guide, Vol. 3, North Atlantic and Mediterranean Weather Analysis and Forecasting Applications, NEPRF Tech. Report 80-07.
- Glover, J.C., 1974: Degradation of resolution in GOES imagery with distance away from the satellite subpoint. Unpublished Manuscript, NOAA/NESS, 4 pp.
- Gyakum, J.R., 1983a: On the evolution of the QE II Storm: Synoptic aspects. *Mon. Wea. Rev.*, **111**, 1137-1155.
- _____, 1983b: On the evolution of the QE II Storm: Dynamic and thermodynamic structure. *Mon. Wea. Rev.*, **111**, 1156-1173.
- Jager, G.L., 1984: Satellite indicators of rapid cyclogenesis., *Mar. Wea. Log*, **28**, 1-5.
- Junker, N.W. and D.J. Haller, 1980: Estimation of surface pressure from satellite cloud patterns. *Mar Wea. Log.*, **24**, 83-87.
- Reed, R.J., and M.D. Albright, 1986: A case study of explosive cyclogenesis in the Eastern Pacific. *Mon. Wea. Rev.*, **114**, 2297-2319.

- Rogers, E., and L.F. Bosart, 1986: An investigation of explosively deepening oceanic cyclones. *Mon. Wea. Rev.*, **114**, 702-718.
- Sanders, F. and J. R. Gyakum, 1980: Synoptic-dynamic climatology of the 'bomb'. *Mon. Wea. Rev.*, **108**, 1589-1606.
- Sheridan, T.F., 1988: Microwave, visual and infrared estimates of precipitation for a rapidly developing eastern North Pacific Ocean cyclone. M.S. Thesis, Naval Postgraduate School, Monterey, Ca., 50 pp.
- Smigielski, F.J. and G.P. Ellrod, 1985: Surface cyclogenesis as indicated by satellite imagery., NOAA Technical Memorandum NESDIS 9, National Oceanic and Atmospheric Administration, U.S. Dept. of Commerce, Washington, D.C., 30 pp.
- Tracton, M.S., 1973: The role of cumulus convection in the development of extratropical systems. *Mon. Wea. Rev.*, **101**, 573-593.
- Troup, A.J. and N.A. Streten, 1972: Satellite-observed Southern Hemisphere cloud vortices in relation to conventional observations. *J. Appl. Meteor.*, **11** 909-917.
- Weldon, R.B., 1977: An ocean cyclogenesis - its cloud pattern interpretation., NWS NESS Satellite Applications Note, 77/7, 16 pp.
- . 1979: Cloud patterns and the upper wind field., Part IV, Satellite Training Course Notes., Applications Laboratory, NESS, Washington, D.C., 52 pp.
- Williams, D.D., 1985: Utilization of satellite-observed cloud patterns to improve analyses of explosive extratropical maritime cyclogenesis. M.S. Thesis. Naval Postgraduate School, Monterey, Ca., 86 pp.

INITIAL DISTRIBUTION LIST

		No. Copies
1.	Defense Technical Information Center Cameron Station Alexandria, VA 22304-6145	2
2.	Library, Code 0142 Naval Postgraduate School Monterey, CA 93943-5002	2
3.	Chairman (Code 63Rd) Department of Meteorology Naval Postgraduate School Monterey, CA 93943-5000	1
4.	Chairman (Code 68Co) Department of Oceanography Naval Postgraduate School Monterey, CA 93943-5000	1
5.	Professor Carlyle H. Wash (Code 63Wx) Department of Meteorology Naval Postgraduate School Monterey, CA 93943-5000	5
6.	Professor Wendell A. Nuss (Code 63Nu) Department of Meteorology Naval Postgraduate School Monterey, CA 93943-5000	2
7.	Lt. Jose F.H. Atangan, USN NOCC JTWC COMNAVMARIANAS Box 12 FPO San Francisco, CA 96630	1
8.	Director Naval Oceanography Division Naval Observatory 34th and Massachusetts Avenue NW Washington, DC 20390	1
9.	Commander Naval Oceanography Command Naval Oceanography Command Stennis Space Center Bay St. Louis, MS 39522	1

- | | | |
|-----|--|---|
| 10. | Commanding Officer
Naval Oceanographic Office
Stennis Space Center
Bay St. Louis, MS 39522 | 1 |
| 11. | Commanding Officer
Fleet Numerical Oceanography Center
Monterey, CA 93943 | 1 |
| 12. | Commanding Officer
Naval Environmental Prediction Research Facility
Monterey, CA 93943 | 1 |
| 13. | Chairman, Oceanography Department
U. S. Naval Academy
Annapolis, MD 21402 | 1 |
| 14. | Chief of Naval Research
800 North Quincy Street
Arlington, VA 22217 | 1 |
| 15. | Office of Naval Research (Code 420)
Naval Ocean Research and Development Activity
800 North Quincy Street
Arlington, VA 22217 | 1 |